Marcela Tatiana Barros Vaz

Degree in Biochemistry

Unraveling phytochemicals with potential therapeutic application for neurodegeneration

Dissertation to obtain a Master Degree in Biochemistry for Health

Supervisor: Regina Menezes, PhD, iBET/ITQB-UNL
Co-supervisor: Cláudia Nunes dos Santos, PhD, iBET/ITQB-UNL

September 2017

Marcela Tatiana Barros Vaz

Degree in Biochemistry

Unraveling phytochemicals with potential therapeutic application for neurodegeneration

Dissertation to obtain a Master Degree in Biochemistry for Health

Supervisor: Regina Menezes, PhD, iBET/ITQB-UNL
Co-supervisor: Cláudia Nunes dos Santos, PhD, iBET/ITQB-UNL

Júri:

Presidente: Prof. Doutor Pedro Matias
Arguente: Prof. Doutor César Mendes
Vogal: Prof. Doutora Margarida Archer

ITQB

September 2017

Acknowledgments

Almost all acknowledgments can't be written or even expressed, the feelings achieved during this journey made me appreciate every single step.

I would like to thank Universidade Nova de Lisboa and ITQB, for this experience.

I'm thankful to Regina Menezes, PhD and Cláudia Nunes dos Santos, PhD supervisor and co-supervisor of this thesis, for the opportunity, also for the time spent discussing ideas and perspectives, for motivation and encouragement.

I felt joyful for having so great master colleagues: Catarina Bastos and Filipa Félix, for being so great friends and staying always with me.

To Rita João Ramos, I really appreciate all your effort since the first day clarifying scientific questions, kindness and perseverance during my journey, it made the difference.

All people that enabled me to develop a new perception of science and acquire a real interest in it: Andreia Gomes, Inês Costa, Inês Figueira, Gonçalo Garcia, Joana Pereira, Vanessa Oliveira, Carolina Jardim and Ana Nunes.

All people mention gave me tools to solve problems, help me to explore the world around me, inspire me and share their knowledge, I would like to express my gratitude and wish you the best.

I am blessed with an incredible best friends, parents and brother, your optimism helps me to expand my horizons and your love made me believe.

To an unexpected gift!

Resumo

Estudos epidemiológicos sugerem que os fitoquímicos podem prevenir e mesmo reverter processos patológicos associados à neurodegeneração. Estudos anteriores revelaram que extratos de folha de *Corema album* protegem as células eucariotas dos efeitos deletérios da expressão e agregação da α-Synucleina e do stress oxidativo na doença de Parkinson. Com o objetivo de identificar o composto bioativo, este extrato foi submetido a um fracionamento bioguiado, que levou a identificação do composto CAL_X. Este estudo mostra que o composto CAL_X reverte a citotoxidade da α-Synucleina, reduz o número de células com agregados de α-Synucleina, assim como modifica o tamanho dos mesmos em modelos de leveduras a expressar α-Synucleina. Do mesmo modo, o extrato da fruta de *Rubus genevieri*, com comprovada bioatividade para esclerose lateral amiotrófica, também foi fracionado, levando à identificação do composto RGE_X. Neste estudo, verificou-se que o composto RGE_X reverte a citotoxidade da proteína FUS, associada a esta doença, através de um mecanismo relacionado com o seu sequestro vacuolar e agregação no citoplasma. Para além de revelar os compostos CAL_X e RGE_X como agentes protetores contra processos patológicos associados à neurodegeneração, este estudo corrobora a relação positiva entre fitoquímicos e neuroprotecção, reforçando a sua utilização como potenciais terapias para estas doenças.

Palavras-Chave: Doença de Parkinson; Esclerose Lateral Amiotrófica; Fitoquímicos; Modelos de Levedura; Neuroprotecção;

Abstract

Epidemiological data suggest that phytochemicals may prevent and even reverse specific pathological processes underlying neurodegenerative diseases. A (poly)phenol-enriched fraction from leaves of *Corema album* was previously reported to modulate central events related to α-Synuclein expression and aggregation as well as oxidative stress in eukaryotic models of Parkinson's disease. In order to identify the potentially bioactive compound, this extract was subjected to a bioguided fractionation, leading to the identification of CAL_X. It is here shown that CAL_X reverses α-Synuclein cytotoxicity, reduces the number of cells displaying α-Synuclein aggregates and modifies the size of aggregates in yeast models expressing α-Synuclein. Likewise, the extract of *Rubus genevieri*, with reported bioactivity towards amyotrophic lateral sclerosis, was also fractionated, leading to the identification of RGE_X. This study reveals that RGE_X reversed FUS cytotoxicity by a mechanism which involves the sequestering of FUS into the vacuole, preventing its cytosolic aggregation. Besides revealing CAL_X and RGE_X as protective molecules for pathological processes associated with neurodegeneration, this study supports the positive correlation between phytochemicals and neuroprotection, reinforcing their use as promising therapeutics.

Keywords: Parkinson's disease; Amyotrophic lateral sclerosis; Phytochemicals; Yeast models; Neuroprotection;

General index

Index of figures

Index of tables

Abbreviations

μ_{max}	Maximum cell growth
A	Final biomass
A30P	Alanine to proline substitution at aSyn residue 30
A53T	Alanine to threonine substitution at aSyn residue 53
Ab	Amyloid beta peptide
ALS	Amyotrophic lateral sclerosis
aSyn	Alpha-synuclein
AUC	Area under curve
BSA	Bicinchoninic acid
CSM	Complete supplement mixture
DHE	Dihydroethidium
DMSO	Dimethyl sulfoxide
DNA	Deoxyribonucleic acid
Dtime	Doubling time
E46K	Glutamic acid to lysine substitution at aSyn residue 46
EDTA	Ethylenediaminetetraacetic acid
ER	Endoplasmic reticulum
fALS	Familial ALS
FCM	Flow cytometry
FUS	Fused in sarcoma
G6P	Glucose-6-phosphate
GAL1	Galactokinase gene
GFP	Green fluorescent protein
h	Hour(s)
HRP	Horseradish peroxidase
iNOS	Induced NOS
Lag	*L*ag phase
LBs	Lewy bodies
LiAc	Lithium acetate
LNs	Lewy neurites
LPS	Lipopolysaccharide
Min	Minute(s)
miRNA	MicroRNAs
NAC	Central hydrophobic non-amyloid
ND	Neurodegenerative diseases
NF-kB	Factor nuclear *kappa B*
nNOS	Neuronal NOS
NO	Nitric oxide
NOS	NO synthase
OD	Optimal Density
OS	Oxidative Stress
P, %	Protection factor
PBS	Phosphate-buffered saline
PD	Parkinson's diseases
PEF	(Poly)phenol enriched fraction
PEG	Polyethylene glycol
PGK	Phosphoglycerate kinase
PI	Propidium iodide
RFP	Red fluorescent protein
RNA	Ribonucleic acid

RNS Reactive nitrogen species
ROS Reactive oxygen species
Rpm Rotations per minute
RRM RNA recognition motif
RT Room temperature
sALS Sporadic ALS
SC Synthetic complete
SC-URA SC without uracil
SDS Sodium dodecyl sulfate
SDS-PAGE SDS polyacrylamide gel electrophoresis
SNCA Synuclein alpha gene
SOD Superoxide dismutase
TBS Tris-buffered saline
TCA Trichloroacetic acid
TE Tris EDTA Buffer
TNF-α Tumor necrosis factor alpha
WT Wild type
YNB Yeast nitrogen base
YPD Yeast extract peptone dextrose

1. Introduction

1.1. Neurodegenerative diseases

Worldwide, demographic aging and genetic factors are leading to an increase of chronic diseases on population, such as Alzheimer's disease (AD), Parkinson's disease (PD), amyotrophic lateral sclerosis (ALS) and Huntington's disease (HD). PD is the most common neurodegenerative movement disorder with a prevalence of 10 million people worldwide, showing an increment with age (1,2). ALS is the most common adult-onset motor neuron disease, with 222,000 cases across the world in 2015 and estimated to increase over the next 25 years (3,4). This disease can affect people of any age although the average onset is 55 years and has a median survival of typically 3-5 years after diagnosis (3). These examples of neurodegenerative diseases (ND) are associated with the irreversible deterioration of the nervous system, including cell dysfunction and death.

1.2. Oxidative stress in neurodegenerative diseases

Reactive oxygen species (ROS) and reactive nitrogen species (RNS) are produced during aerobic respiration, cellular metabolism and defense against pathogens. The primary source of these radical species is mitochondria during the electron transport chain. The endoplasmic reticulum (ER), peroxisomes and cytosol may also contribute to their production (5). Exogenous factors are also sources of these reactive molecules, such as xenobiotics, bacterial infection and ionizing radiation. At physiological concentrations, ROS and RNS, play important regulatory and mediator functions. Their accumulation leads to the state known as oxidative stress (OS), which increases the risk of damage to biological molecules implicated in a variety of processes in living organisms (6,7). ROS can induce lipid peroxidation as well as the disruption of membrane lipid bilayer. The interaction with proteins may occur in a variety of ways including fragmentation of the peptide chain, alteration of electrical charge, cross-linking, oxidation of specific amino acids and protein aggregation. DNA can also be affected by ROS damage, which may result in alteration of gene expression. These processes lead to cell and tissue injury, however, the cell's antioxidant mechanisms limit the accumulation of free radicals and balance the integrity of biological systems (**Fig.I.1**) (8,9). The activation of enzymatic antioxidant defenses include superoxide dismutase (SOD), glutathione peroxidase, catalase and peroxiredoxins whereas non-enzymatic antioxidants include ascorbic acid (vitamin C), α-tocopherol (vitamin E), glutathione, carotenoids, and (poly)phenols (10,11). Under pathological conditions, the antioxidant systems are not enough to counteract the excessive production of ROS/RNS leading to an imbalance in favor of the oxidants. This is particularly susceptible to happen in the brain, due to its intense oxygen consumption, weak antioxidant mechanisms and high lipid content (12,13). Indeed, clinical and preclinical studies have shown higher ROS levels and antioxidant defense markers in the plasma, serum, cerebral tissue and cerebrospinal fluid samples of ND patients as compared to healthy controls (14,15).

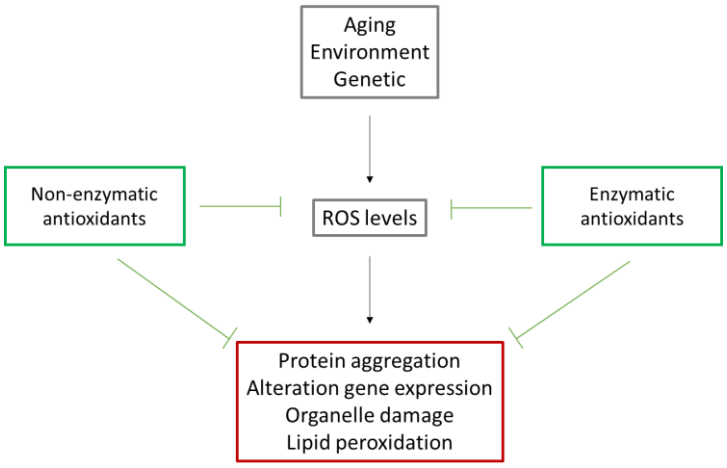

Figure II.1 - Reactive oxygen species (ROS) homeostasis in eukaryotic systems. A variety of stimulus triggers the increase of ROS levels leading to protein aggregation, alteration of gene expression, organelle damage and lipid peroxidation. The antioxidant mechanisms are activated to reestablish ROS levels and prevent damage of biological systems. The inability of cells to restore ROS homeostasis lead to pathological processes associated with several diseases, particularly neurodegeneration.

Protein misfolding is largely associated with a number of disorders, including NDs. Misfolded proteins can deposit extracellularly as amyloid plaques and aggregates or amyloid-like structures can be found inside the cells (16). Amyloid fibrils consist of highly ordered beta sheet-rich structures, made up of polymeric fibrils, **Fig. I.2**. The toxicity of these highly organized fibrils can be associated both with a loss of function of disease proteins or with a gain of function of the intermediate species formed during the process of self-assembly (16,17). The exact cytotoxic species is in question, however, the mature fibril species are currently believed to be less toxic than the oligomeric aggregates (18). Despite the well-established links demonstrating the role of aggregates in the dysregulation of cell signaling, oxidative stress, inflammation, apoptosis, and other cellular abnormalities, the mechanisms through which aggregation-prone proteins cause neurodegeneration remain unclear (19,20).

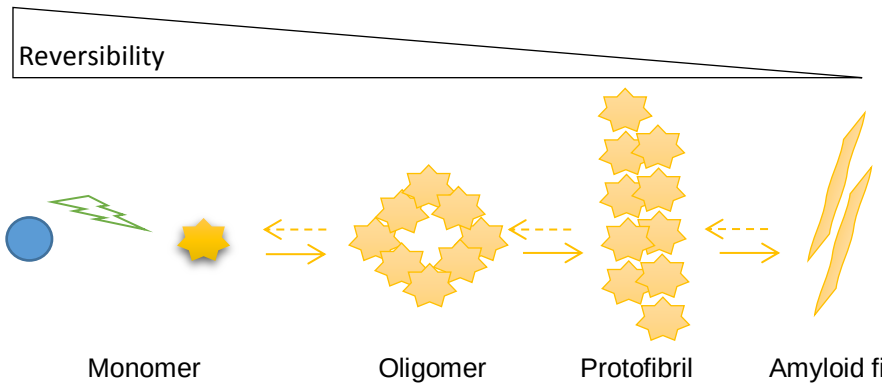

Figure I.2 – Schematic representation of amyloid fibril formation. The reversibility in each step of fibril formation is indicated (Adapted from Huang *et al*, 2013).

1.4. Parkinson's disease

James Parkinson first described PD as a neurological syndrome in 1817 (21). Clinical manifestations consist of severe motor defects characterized by resting tremor, muscle rigidity, bradykinesia and postural instability (22). In addition, there are non-motor characteristics like cognitive impairment, depression, olfactory deficits and psychosis (22). At the molecular level, PD is characterized by the loss of dopaminergic neurons in *substancia nigra pars compacta* (22).

Protein cytoplasmic inclusions in the surviving neurons, known as Lewy bodies (LBs) and Lewy neurites (LNs), are the typical pathological hallmark in familial and sporadic PD and other synucleinopathies (22). The major component of these insoluble proteinaceous inclusions are unfolded aSynuclein (aSyn), which adopts a fibrillar morphology (23). Environmental factors, such as exposure to pesticides or metals, are thought to increase the risk for PD and, possibly, other synucleinopathies.

1.4.1. aSynuclein

aSyn is a soluble 140-residues protein abundant in nerve terminals that plays a central role in PD. Missense mutations (A53T, A30P, E46K) and duplications of *SNCA* locus were associated with familial cases of PD (24). Mutations in Parkin, DJ-1, PINK1, LRKK2 and ATP13A2 have been also shown to cause familial PD (24,25). Later, the aSyn gene was implicated in sporadic cases of the disease, demonstrating a causative role. The exact role of aSyn remains poorly understood, however it has been considered as a neurotransmitter release (26).

The cellular mechanisms triggering aSyn aggregation are not clear and neither is the relationship of aSyn aggregation with PD pathology. Several theories attempt to explain the toxicity of misfolded/aggregated aSyn, including the impairment of the ER to Golgi trafficking, dysfunction of mitochondria and blocking of protein clearance mechanisms (27,28). The precise nature of the toxic aSyn species is still unclear (29,30).

1.5. Amyotrophic lateral sclerosis

ALS is also referred to as Charcot's disease, due to the man who diagnosed the first cases of ALS in 1874.

ALS is characterized by the progressive degeneration of upper and lower motor neurons in the brain and spinal cord (31). The involvement of different sets of motor neurons or different regions of the body might result in spasticity, muscle wasting, and weakness, leading to paralysis, and difficulties in speech, swallowing and breathing (32).

The central pathological hallmark of ALS is the presence of cytoplasmic inclusions in degenerating motor neurons and surrounding oligodendrocytes (33). The aggregates found in ALS patients are classified as Lewy body-like hyaline inclusions that are predominantly composed by ubiquitinated proteins (33).

The distinction between familial and sporadic ALS is not obvious because mutations linked to familial ALS (fALS) had been occasionally identified in patients with apparent sporadic ALS (sALS). There are a variety of genes implicated in the ALS pathogenesis, which can be

grouped into several categories: those varying superoxide metabolism (*SOD*); those altering proteostasis and protein quality control (*OPTN*); those affecting RNA stability, function and metabolism (*FUS* and *TARDBP*); and those perturbing cytoskeletal dynamics in motor neurons (*DCTN1*) (34–36). The first mutations associated with ALS were detected in SOD1, which encodes the ubiquitously expressed copper/zinc superoxide dismutase. About 20% of fALS cases are caused by mutations in this gene (34). FUS/TLS (**F**used in **s**arcoma or **t**ranslocated into **s**arcoma) mutations are associated with some of the most aggressive phenotypes of the disease (37,38). A series of genetic studies have shown that FUS mutations account for 5 % of fALS and 1% of sALS cases (39,40).

1.5.1. FUS

FUS is a RNA-binding protein that is encoded by the *FUS* gene in humans and has been implicated in the pathogenesis of both myxoid liposarcoma and low grade fibromyxoid sarcoma, hence the name (41). FUS is a member of the heterogeneous nuclear ribonucleoproteins that regulates DNA and RNA metabolism, regulation of pre-mRNA, transcription, RNA splicing, miRNA processing, export to the cytoplasm and could play a role in the modulation of synaptic activity (39,42).

The role of FUS in ALS remains to be determined. However, both gain- and loss-of-function mechanisms have been proposed. The toxic gain of function may relate to the traffic and formation of intracellular aggregates whereas the loss of nuclear function may lead to a defective regulation of direct FUS-RNA targets (43–45).

1.6. *Saccharomyces cerevisiae*: a powerful model for pathological processes of neurodegenerative diseases

S. cerevisiae is a unicellular microorganism and as the simplest eukaryotic organism, it presents some advantages over more complex models: it has a short generation time, it is easily handled under experimental conditions and cultured under almost inexpensive conditions. The fundamental biological processes of life are highly conserved between yeast and humans allowing recapitulating the pathological pathways of many diseases. Particularly, processes such as protein quality control, vesicular trafficking and secretion, autophagic pathways, unfolded protein response, and mitochondrial biogenesis and metabolism are highly conserved (46,47).

S. cerevisiae was the first eukaryotic organism to have its genome fully sequenced in 1996 (48,49). With unique available genetic and biochemical tools, yeast has proven to be a valuable system to study the function of human proteins involved in many disorders. If the genes of interest have a yeast homolog is possible to delete or overexpress those genes, and fuse them to a tag such as GFP, facilitating protein localization assays and expression analysis. Otherwise, when the yeast genome does not encode homologues of human disease genes, functional

analysis can still be performed via heterologous expression, as it happens in the aSyn and FUS yeast models (50,51).

The expression of aSyn in yeast results in the formation of cytosol inclusions and induces OS, possibly due to aSyn-mediated mitochondrial dysfunction (27). It also affects vesicular trafficking, impair of proteasomal activity, and promotes disturbances in lipid metabolism (51), as in mammalian cells. The human aSyn includes three main regions: the N-terminus with the amphipathic region as a binding site to phospholipid membranes; a central hydrophobic nonamyloid (NAC) component region, important for filament assembly during disease pathogenesis; and an acidic ligand binding in region COOH-terminal (**Fig. I.3**) (52).

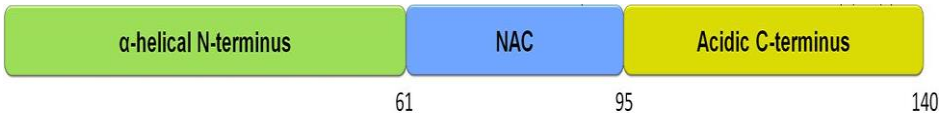

Figure I.3 - Schematic representation of aSyn protein domains. The amphipathic region, the central hydrophobic non-amyloid (NAC) domain, and the acidic COOH-terminal region are indicated, adapted from http://journal.frontiersin.org/article/10.3389/fgene.2014.00382/ful.

The yeast model of FUS expression recapitulates multiple features of ALS pathology: FUS nuclear to cytosolic translocation, the formation of cytosolic aggregates and cell growth inhibition (50). In yeast, FUS aggregation and toxicity depends on the N-terminal region of the protein containing the RNA recognition motif (RRM) and the first arginine/glycine rich region (Arg, Gly) domain, being the N-terminal and the last Arg, Gly domain responsible for the toxicity (**Fig. I.4**) (33).

Figure I.4- Schematic representation of FUS protein domains. The RNA recognition motif (RRM) and the arginine/glycine rich region are indicated, adapted from http://journal.frontiersin.org/article/10.3389/fncel.2015.00423/full

1.7. Properties of phytochemicals against neurodegeneration

Plants synthetize phytochemicals required for maintenance of plant cells. They have been identified as a source of exogenous modulators of antioxidants responses constituting a promising strategy to delay or prevent oxidative damage. However, only a few have been shown to be therapeutically useful *in vivo* due to absorption, distribution, metabolism, storage and excretion (53). The main phytochemicals occurring in plants consumed by humans as foods, are phenolics, terpernoids, alkaloids, organosulphur compounds and carotenoids. The phenolic compounds are classified into five major groups: phenolic acids, flavonoids, lignans, stilbenes and tannins (**Fig. I.5)** (53). They show a structure composed of a phenol group with at least one aromatic ring with one or more hydroxyl groups connected.

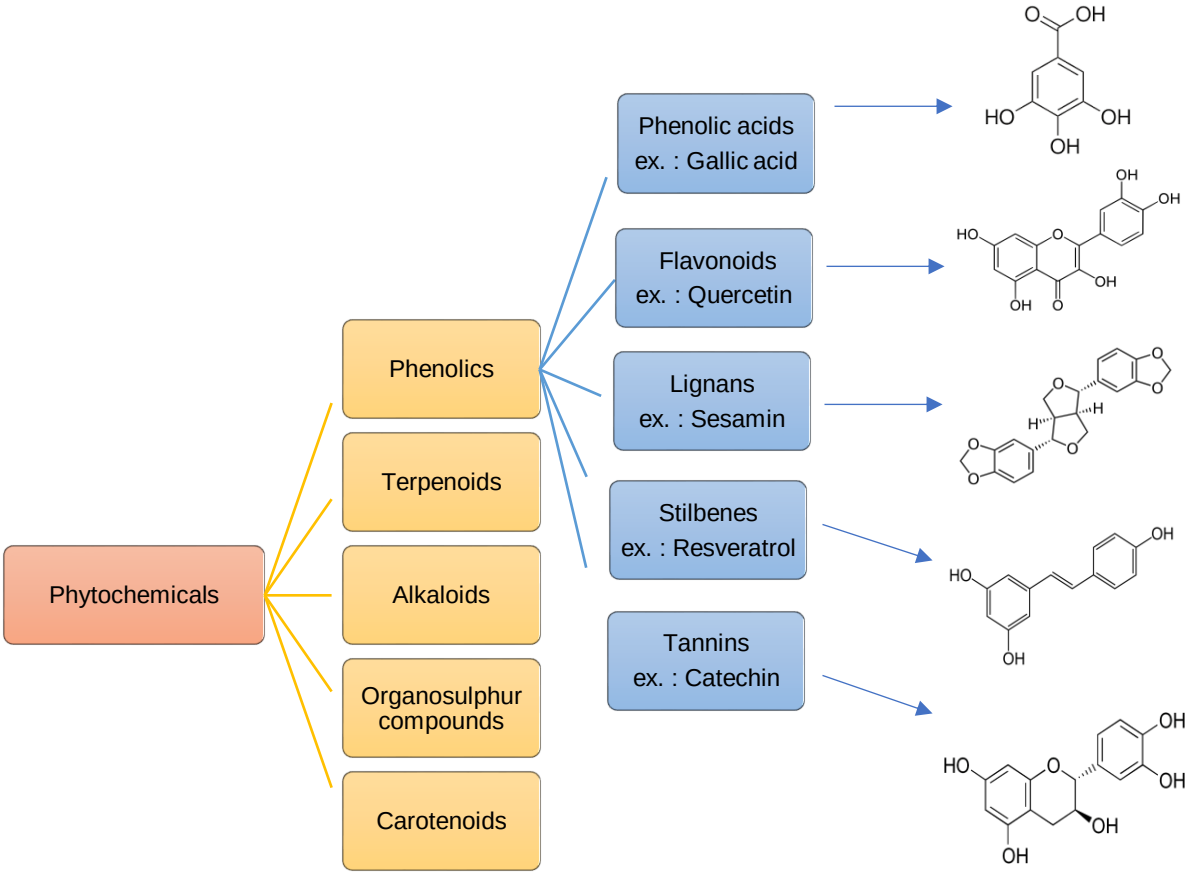

Figure I.5- Phytochemicals classification (Adapted from Dixon and Alxous, 2014 and HMBD).

Several natural phytochemicals play important roles in reducing the incidence of amyloid diseases, inhibiting the production and deposition of amyloidogenic peptides, increasing enzymatic antioxidant activity, inducing autophagy, attenuating inflammation, displaying radical scavenging activities and metal chelating properties (55–58).

1.7.1. Bioactive compounds from *Corema album*

The extract from *Corema album* leaf (Portuguese crowberry) was identified in previous studies as bioactive against the pathological processes associated with PD (59). To identify the compound(s) associated with the bioactivity, this extract was subjected to a bioguided fractionation in the framework of the BacHBerry project (60). This procedure led to the identification of two fractions that retained the bioactivity of the original extract as evaluated by growth curve analysis. The fractions were analyzed by LC-MS and a list of putative identities was defined. Some compounds were discarded based on previous studies (59 and unpublished data) and genipin (referred to as CAL_X in the abstract for confidentiality reasons) emerged as a potential bioactive compound. Interestingly, genipin was previously reported as a potential bioactive improving neurodegenerative diseases (61).

The iridoid monoterpene genipin has a molecular weight of 226.226 g/mol. It is a hydrolyzed metabolite of geniposide by β-D-glucosidases, the original compound present in plants (62). The potential biotechnological applications of genipin are associated with its property as a natural cross-linker for proteins and collagen (63). Its chemical structure is presented in **Fig I.6.**

Genipin has been reported to possess anti-inflammatory and a direct free radical scavenger activity (64,65). Its pharmacological actions have been associated with the inhibition of iNOS expression, TNF-α and NO production as well as inhibition NF-kB signaling in lipopolysaccharide (LPS)-stimulated macrophages and BV-2 cells (66,67). In rat hippocampal neurons, genipin emerged as a potential candidate for the treatment of AD via reduction of amyloid beta protein (Ab) toxicity, the major constituent of amyloid plaques in AD (68,69). The bioactivity of geniposide has been associated with the improvement of PD clinical manifestations and restoration of tyrosine hydroxylase positive dopaminergic neuron in the *substantia nigra pars compacta* (70). Geniposide antagonizes cytotoxicity induced by Ab exposure, oxidative stress, endoplasmic reticulum stress, and inflammatory reactions, which appear to be important in the pathogenesis AD and inflammation (65,66). Nevertheless, it has been claimed that genipin exerts a higher protective action towards inflammatory processes and prevention of Ab toxicity than geniposide (68,72).

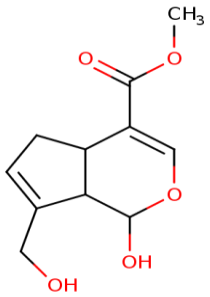

Figure I.6-Chemical structure of genipin (Adapted from HMBD).

1.7.2. Bioactive compounds from *Rubus genevieri*

In the framework of the BacHBerry project, the extract from *Rubus genevieri* fruit (blackberry) was identified as a potent protectant against the pathological processes associated with ALS, using yeast models expressing FUS (60). A similar bioguided fractionation procedure was conducted aiming to identify the bioactive compound(s). Twenty-eight fractions were obtained and re-tested in yeast, leading to the identification of three bioactive fractions. Chemical profiling by LC-MS was pursued and corilagin (referred to as RGE_X in the abstract for confidentiality reasons) was the only compound presented in more than one bioactive fractions.

Corilagin is a member of the (poly)phenolic ellagitannins family. It has relatively high hydrophilicity and large molecular weight, 634.455 g/mol. The chemical structure is shown in **Fig. I.7.** Little research has been performed on the activity of corilagin. Some data indicate that corilagin acts as neurotoxic suppressor of inflammatory mediators, such as TNF-α, NO, interleukins and as a repressor of NF-kB activation, attenuating Ab-induced inflammatory responses and protecting cells from Ab-induced damage and apoptosis (74,75). Corilagin has been also described as an anti-apoptotic and free radical scavenging compound, decreasing intracellular ROS and increasing SOD activity (76,77). In animal models, corilagin has shown anti-inflammatory properties via intraperitoneal injection, which was not observed via oral administration (78). Despite the reported action of corilagin towards oxidative stress and neurodegeneration, its protective role for ALS has not yet been explored. The bioactivity identified in the scape of the BacHBerry project emphasizes the need to investigate deeper the molecular mechanism underlying corilagin action as to provide the foundation for novel ALS therapeutic strategies.

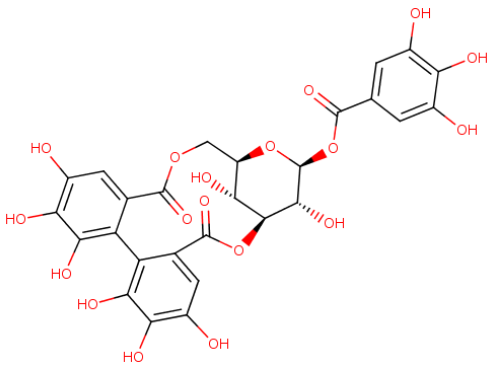

Figure I.7- Chemical structure of corilagin (Adapted from HMBD).

1.8. Goals

Neurodegenerative disorders, including PD and ALS, cause a huge societal and economical burden mostly because there is no cure for these diseases, also because they are highly debilitating, requiring extensive specialized patient care. It is therefore imperative to identify novel lead molecules targeting the associated pathological processes. Yeast models of PD and ALS were used in an attempt to identify the bioactive compounds from *C. album* and *R. genevieri,* respectively, and to characterize the molecular mechanism underlying cellular protection. The following goals were pursued:

1-Validation of genipin and corilagin as protective compounds for PD and ALS, respectively;

2-Investigation of the molecular mechanisms underlying cellular protection by genipin;

3-Identification of corilagin cellular targets.

The strategy used to achieve these goals is summarized in figure Fig.I.8

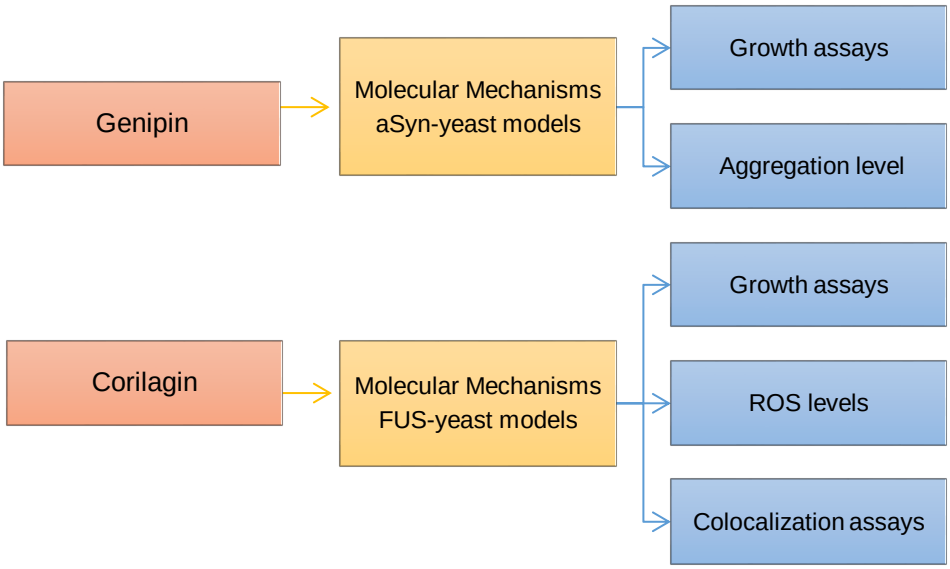

Figure I.8- The strategy used to evaluate the role of genipin and corilagin for PD and ALS pathological processes, respectively.

2. Material and methods

2.1. Material

Acrylamide, glycine and TRIS were purchased from Carl Roth, Germany. Ammonium persulfate (APS) was purchased from Biosciences, USA. Anti-aSyn mouse polyclonal antibody was purchased from Santa Cruz biotechnology. Goat anti-mouse and goat anti-rabbit antibodies were purchased from Pierce, USA. Mouse anti-PGK antibody was purchased from Invitrogen USA. Anti-FUS rabbit monoclonal antibody was purchased from Millipore, USA. Complete protease inhibitor tablets [ethylenediaminetetraacetic acid (EDTA) free] and phosphatase inhibitor: PhosSTOP were purchased from Roche Applied Sciences, UK. Complete supplement mixture (CSM) and CSM-URA (uracil) were purchased from MP biomedicals, USA. Protein marker VI and sodium chloride (NaCl) were purchased from Panreac Aplichem. Corilagin and genipin were purchased from Carbosynth, UK. Dimethyl sulfoxide (DMSO) was purchased from Duchefa Biochemie, Netherlands. Acetone was purchased from Fluka biochemika, Germany. ECL was purchased from GE Healthcare, UK. Agar and yeast extract were purchased from Himedia, India. Galactose, glass beads, glucose, glycerol, hydrogen chloride (HCl), hydrogen peroxide (H_2O_2), lithium acetate (LiAc), polyethylene glycol (PEG), raffinose, salmon sperm (Deoxyribonucleic acid, single stranded), trichloroacetic solution (TCA) and tween 20 were purchased from Sigma, USA and Germany. Micro bicinchoninic acid (BCA) kit was purchased from Thermo scientific, USA. EDTA was purchased from VWR. Sodium dodecyl sulfate (SDS), tetramethylethylenediamine, Ponceau and potassium chloride (KCl) were purchased from Merck Germany. Yeast nitrogen base (YNB) without amino acids and bactopeptone was purchased from BD Dicfo, USA.

2.1.1. Compound aliquots

Aliquots of 100 mM were prepared and stored at -20 ºC. 433 µL DMSO were added per 10 mg of genipin powder (98% purity). 155 µL DMSO were added per 10 mg of corilagin powder (98% purity).

2.2. *Saccharomyces cerevisiae* strains and growth conditions

The yeast strains and plasmids used in this study are listed in **Table II.1**.

Table II.1- Yeast strains used in this study.

Yeast strain	Genotype	Reference
W303-1A	*MATa can1-100 his3-11,15 leu2-3,112 trp1-1 ura3-1 ade2-1*	(79)
W303-1A_UT	W303-1A *trp1-1::TRP1 ura3-1::URA3*	(51)
aSyn	W303-1A *trp1-1::GAL1pr-SNCA(WT)-GFP TRP1;ura3-1::GAL1pr-SNCA(WT)-GFP::URA3*	(51)
W303-1B	*MATα can1-100 his3-11,15 leu2-3,112 trp1-1 ura3-1 ade2-1*	(79)
FUS	W303-1B *his3-11,15::GAL1 FUS*	(unpublished data)
W303-1B_H	W303-1B *his3-11,15::HIS3*	(unpublished data)
BY4741	*MATa his3Δ1 leu2Δ0 met15Δ0 ura3Δ0*	(80)
SEC13-RFP	*MATa his3Δ1 leu2Δ0 met15Δ0 ura3Δ0 SEC13-RFP*	(81)
BY4742	*MATα his3Δ1 leu2Δ0 lys2Δ0 ura3Δ0*	(80)
ZRC1-mCherry	*MATα his3Δ1 leu2Δ0 lys2Δ0 ura3Δ0 ZRC1-mCherry*	(81)

The W303-1A yeast strain carrying two integrated copies of the fusion gene *SNCA*-GFP under regulation of the *GAL1* inducible promoter was used to investigate the role of genipin on aSyn proteotoxicity; it was referred to as aSyn strain. The W303-1A_UT was used as the empty strain.

The W303-1B yeast strain carrying one integrated copy of *FUS* under regulation of *GAL1* was used to investigate the role of corilagin on FUS proteotoxicity; it was referred to as FUS strain. The strain W303-1B_H was used as the empty strain.

The GFP-FUS fusion gene under the regulation of the inducible *GAL1* promoter was encoded by pYES2 plasmid (pYES2_GFP-FUS), with a corresponding empty vector (pYES2_CT) (50). These plasmids were transformed into BY4741 and BY4742. Cells encoding pYES2_GFP-FUS were designated as BY4741_GFP-FUS and BY4742_GFP-FUS, respectively. Cells encoding the empty vector pYES2_CT were referred to as W303-1A, BY4741 and BY4742.

For the co-localization assays, the plasmid pYES2_GFP-FUS was expressed in the strains BY4741_SEC13-RFP and BY4742_ZRC1-mCherry originating the strains named BY4741_SEC13-RFP_GFP-FUS and BY4742_ZRC1-mCherry_GFP-FUS strains. The pYES2_CT was used to originate the respective empty strains: BY4741_SEC13-RFP and BY4742_ZRC1-mCherry (50).

2.3. Yeast growth conditions

All strains were thawed from glycerol stocks at -80ºC [Yeast extract peptone dextrose (YPD) liquid medium: 1% (w/v) Yeast extract; 2% (w/v) bactopeptone; 2% (w/v) dextrose-glucose; 50% (v/v) glycerol], streaked onto agar-YPD plates [YPD liquid medium; 2% (w/v) agar] and incubated for 48 h at 30ºC. Single colonies were streaked onto fresh agar-YPD plates and

incubated for further 48 h at 30ºC, **Fig. II.1**. The plates could be stored at 4ºC for one month, after which single colonies were re-streaked onto agar-YPD plates.

For all experiments, a pre-inoculum was prepared in synthetic complete medium (SC) [0.79 g.L^{-1} complete supplement mixture (CSM); 0.67 g.L^{-1} yeast nitrogen base (YNB); 1% (w/v) raffinose]. From the agar-YPD plates, one single colony was inoculated in 3 mL of SC-raffinose medium and cells were grown overnight at 30ºC under an orbital agitation at 200 rpm (Agitorb 200 IC, Norconcessus, Portugal). The optical density (OD) at 600 nm (OD_{600}) of cultures was measured (Plate spectrophotometer Power Wave XS, Biotek) and cultures were diluted in fresh SC-raffinose medium to obtain a culture with a final OD_{600} = 0.2 after *t* h, according to the following equation:

$$ODi \times Vi = \frac{ODf}{2^{\left(\frac{t}{gt}\right)}} \times Vf$$

Where OD_i = initial optical density of the culture, *Vi* = initial volume of culture, OD_f = final optical density of the culture, *t* = time (h), g_t = generation time of the strain, V_f = final volume of culture.

The cultures were centrifuged at 2000 *g* for 5 min, resuspended in SC-galactose [0.79 g.L^{-1} CSM; 0.67 g.L^{-1} YNB; 2% (w/v) galactose] medium and incubated for 6 h at 30°C (**Fig.II.1**). OD_{600} readings were performed in the plate spectrophotometer Power Wave XS, Biotek. For cells expressing the plasmids**,** the cultures were grown in SC-URA medium [0.77 g.L^{-1} CSM-URA; 0.67 g.L^{-1} YNB], containing the appropriate carbon sources.

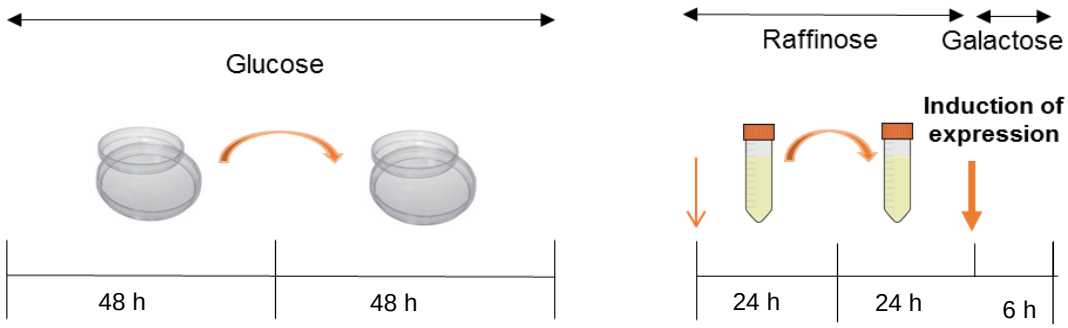

Figure II.1- Schematic representation of the growth conditions. Glucose was used as the primary carbon source for yeast growth. Raffinose was used to relieve glucose repression and galactose was used as an inducer of *GAL1* promoter-driven expression.

2.4. Preparation of competent yeast cells

A single colony was inoculated in 4 mL of YPD and cultures were incubated overnight at 30ºC under orbital agitation. Cultures were diluted to OD_{600} = 0.1 in 10 mL of fresh YPD and incubated for 3.5 h at 30ºC as indicated above. Cultures were centrifuged for 5 min at 3270 *g*, the

supernatant was removed, and the pellet was washed and centrifuged for 1 min at 3270 *g*. The cells were resuspended in 1 mL of TE/LiAc [10 mM Tris-HCl; 1mM EDTA, pH 7.5; 1 M Lithium Acetate pH 7.5], centrifuged as above and resuspended in 200 µL of TE/LiAc.

2.5. Transformation of yeast cells

The transformation mixture was prepared as follows: 5 µL of denaturated DNA from salmon sperm; 2 µL of plasmid DNA; 50 µL of competent cells, 300 µL of PEG/TE/LiAc [40% polyethylene glycol (PEG); 100 mM LiAc in 1xTE]. Cell suspensions were incubated for 30 min at 30ºC, and subjected to thermal shock for 20 min at 42ºC. Finally, cells were washed with water, centrifuged and spread onto agar SC-URA. Plates were incubated for 48 h at 30ºC.

2.6. Growth assays

Growth curves were performed with the indicated concentrations of both compounds in "Nunc" 96-well plate. First, the compounds and the appropriated medium (SC galactose and glucose or SC-URA galactose and glucose) according to the strain used, were transferred to the microplate. The volume of yeast cultures required to obtain an inoculum with an ODfinal of OD_{600} = 0.03 (as described in section **2.3**) was then prepared. The plates were incubated at 30ºC for 24 h, with constant shaking and yeast growth was monitored hourly by OD_{600} readings in a spectrophotometer microplate reader (PowerWave XS Biotek and Synergy HT). The data was treated using R software.

2.6.1. Data extraction from the growth curves

All experiments were performed with 9 replicates (3 technical x 3 biological). Raw ODs were subtracted by the correspondent blank value to give the corrected OD_{600} values, and technical replicates corrected OD_{600} values were averaged. Mean corrected OD_{600} data were divided by the minimum OD_{600} value and then transformed applying the natural logarithm. The R script (R studio Version 1.0.136) was used to adjust a model-based, using nonlinear parametric regression. The growth parameters were estimated from the best model fit: (1) maximum cell growth (*µmax*), (2) length of the lag phase (lag, *λ*) and (3) the area under curve (AUC). The cell doubling time (*Dtime*) at maximum cell growth was calculated by ln (2) */ µmax*. The final biomass (*A*) was estimated by reading through OD_{600} after 24 h. In addition, lower and upper confidence limits for the model-based fits were calculated at the 95% confidence level. The adjusted model and corresponding points were represented graphically to compare the conditions under study. Protection factor (P, %) was calculated as:

$$P(\%) = \frac{AUC(compound) - AUC(disease)}{AUC(empty) - AUC(disease)}$$

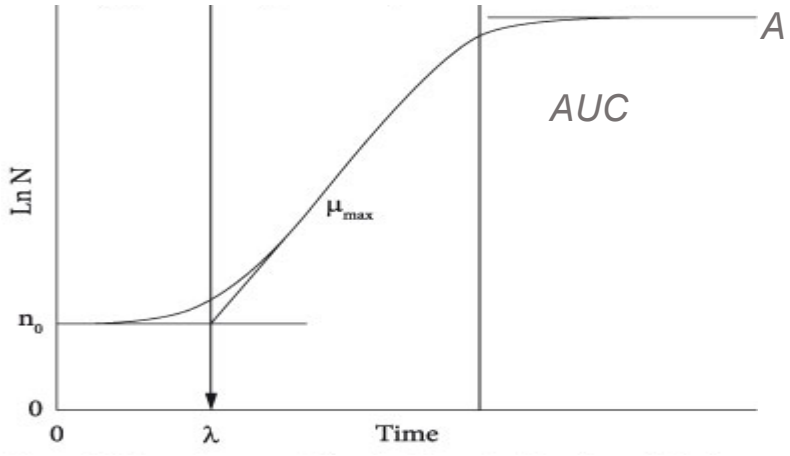

Figure II.2- Hypothetical growth curve of yeast cultures. The growth parameters: final biomass (*A*), maximum cell growth (μ_{max}), lag time (λ) and area under the curve (AUC) are indicated (Adapted from Swinnen *et al*, 2004)

2.7. Fluorescence microscopy

Fluorescence microscopy was used to evaluate aSyn and FUS aggregates as well as FUS compartmentalization. After 6 h induction of aSyn and FUS expression in the presence or absence of the compounds, 500 µL of cells were collected by centrifugation at 2000 *g* for 2.5 min. Cell pellets were washed with 500 µL of phosphate-buffered saline (PBS) and centrifuged at the same conditions. Slides were prepared using 4 µL of cells suspension. GFP and mCherry fluorescence was visualized in living cells using a fluorescence microscope (Leica DM6B widefield with a cooled CCD camera, Roper Scientific Coolsnap HQ and Leica Application Suitex software version 1.90.13747). At least 500 cells per condition were manually counted, using Fiji-ImageJ software.

2.8. SDS-PAGE and immunoblotting

aSyn-GFP and FUS expression were induced for 6 h in SC galactose medium supplemented or not with compounds. For total protein extraction, cells were collected by centrifugation; the pellet was washed with water, resuspended in TCA solution [10% (v/v) triclocroacetic acid solution] and cell suspensions were incubated for 20 min at -20ºC. Cells were centrifuged for 3 min at 15 000 *g*, the pellet was washed with acetone, air-dried, and cells were lysed in MURB buffer [50 mM sodium phosphate; 25 mM MES; pH=7.0, 1% (w/v) SDS; 3 M urea; 0.5% (v/v) 2-mercaptoethanol; 1 mM sodium azide; supplemented with protease inhibitor (complete protease inhibitor tablets, EDTA free) and phosphatase inhibitor: PhosSTOP] by vortexing (3 cycles of 30 s in the vortex and 5 min on ice) using acid-washed glass beads. Cell debris were removed by centrifugation at 10 000 *g* for 1 min at room temperature (RT) and the supernatant was collected.

Equal amounts of total protein, normalized by OD_{600}, were heated for 10 min at 70ºC before being resolved by SDS-PAGE (12% gels, 200 V, for 45 min). The protein marker VI, 10-245 kDa range, was used as a protein marker.

Under certain conditions, cells were isolated using TBS buffer supplemented with protease and phosphatase inhibitors. Protein extracts were sonicated for 1 min and protein concentrations were estimated using the micro BCA kit according to the manufacturer's instructions. Protein samples were mixed with 4x protein sample buffer [0.24 M Tris pH=6.8; 5% (v/v) 2-mercaptoethanol; 8% (w/v) SDS; 40% (v/v) glycerol; 0.1% (w/v) bromophenol blue].

Gels were transferred onto nitrocellulose membranes using a trans-blot turbo transfer system for 7 min at 25 V for each mini gel, as specified by the manufacturer. Membranes were incubated with ponceau S stain for 1 min followed by destaining with water to monitor the transfer procedure.

Immunoblotting was performed following standard procedures. The blocking procedure was performed by incubation with 5% (w/v) non-fat dry milk in TRIS-buffered saline (TBS pH=7.6) for 45 min at RT. The membranes were incubated, overnight at 4ºC, with the primary antibody diluted in 5% (w/v) BSA in TBS, as follows: anti-aSyn and anti-FUS were diluted to a final concentration of 1:1000 and anti-PGK (phosphoglycerate kinase) was diluted to a final concentration of 1:5000. The membranes were washed three times with TBST [TBS; 0.1% (v/v) Tween 20] for 10 min each, followed by incubation with secondary antibody, anti-mouse HRP conjugated or anti-rabbit HRP conjugated diluted in 5% (w/v) non-fat dry milk in TBST for 2 h, diluted to a final concentration of 1:5000. After wash with TBST three times, protein signals were developed with ECL solution (82).

When required, membranes were subjected to mild-striping conditions as follows: membranes were incubated for 10 min in striping buffer [1,5 g glycine; 1% (w/v) SDS; 0,1% (v/v) Tween 20; pH=2.2 in 100 mL miliQ water], washed three times with TBS for 10 min with agitation; and blocked as indicated above. Images were acquired using Chemidoc XRS+ and the intensity of protein signals was evaluated using the Image J software 1.8.0_66. Specific protein signals were normalized against the PGK signal.

2.9. Filter trap

Total proteins were isolated using TBS buffer supplemented with protease and phosphatase inhibitors as indicated in section **2.8.** Protein extracts were sonicated and protein concentration was estimated using micro BCA kit according to the manufacturer's instructions. First, 25 µg of total protein were mixed with 1% (v/v) SDS/PBS.The nitrocellulose membrane (pore size 0.2 µm) was soaked in 1% (v/v) SDS/PBS and the samples were applied to a dot blot apparatus and filtered by vacuum. The membrane was washed twice with 1% (v/v) SDS/PBS (83,84). Immunoblotting was performed as described in section **2.8**.

2.10. Flow Cytometry

Flow cytometry was performed in a CyFlow Cube6 with CyView, equipped with blue laser: 488 nm. To determine superoxide levels, cells were incubated with 30 µM DHE for 15 min at 30°C, with agitation and protected from light. As a positive control, cells were incubated with 500 mM hydrogen peroxide. To determine cell viability, cells were incubated with 5 µM propidium iodide for 15 min at 30°C, with agitation and protected from light. Cells boiled for 10 min were used as a positive control. A minimum of 10 000 events were collected for each experiment. Data analysis was performed using the FlowJo software 10.0.7r2. Results were expressed as mean fluorescence intensity for DHE and by frequency of parent cells for PI.

2.11. Statistical Analysis

Statistical analyses were performed using Prism 6 (GraphPad Software, version 6.01). All data are reported as averages of at least three independent measurements ± standard deviation (SD). Different statistical tests were performed according to the statistical data. Statistic significant were considered when *p value ≤ 0.05, **p value ≤ 0.01, ***p value ≤ 0.001.

3. Results and Discussion

3.1. Effect of genipin on the growth of aSyn strain

The bioactivity of genipin towards PD pathological processes was assessed using the yeast model of aSyn-GFP aggregation and toxicity (51). Cell growth was monitored for 24 h in SC-glucose (control condition – aSyn OFF) and SC-galactose (aSyn ON) media supplemented or not with genipin to a final concentration of 10, 30, 50, 70 µM. These concentrations were showed to be non-toxic for the W303-1A_UT empty strain as assessed by the area under the curve (AUC) values (**Fig.III.1B**). The expression of aSyn-GFP led to a decreased growth in comparison with the W303-1A_UT and only the treatment with 10 µM genipin restored cellular growth, as shown in **Fig.III.1A**. Extraction of growth parameters using "R" script indicated that treatment of the aSyn-GFP strain with 10 µM genipin reduces the lag time of the cultures, which impacts on the final biomass and on the AUC **Fig.III.1B**. The AUC parameter was then used to calculate the protection factor of genipin, 78.3% **(Fig.III.1C)**. Taking into consideration that genipin was added to cultures concomitant with induction of aSyn-GFP expression, these data suggest that genipin may interfere with the formation of toxic intracellular aggregates, allowing cells to rapidly recover cellular growth after exposure to galactose medium, i.e., after induction of aSyn expression.

A

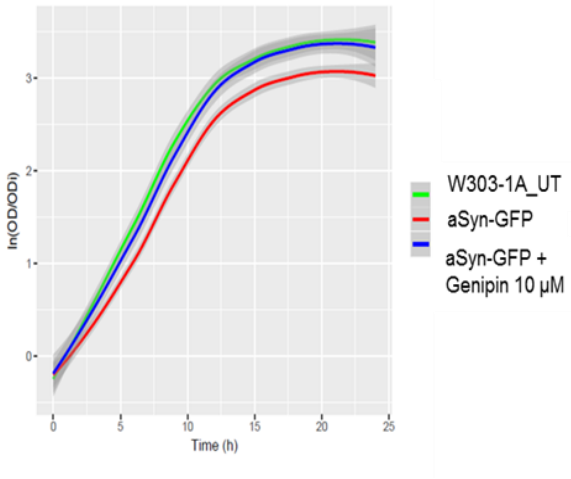

C

Condition : Genipin	Protection factor %	P_Lower bound	P_Upper bound
10 µM	78.3	15.9	107.6
30 µM	--	--	22.2
50 µM	--	--	23.8
70 µM	--	--	24.3

B

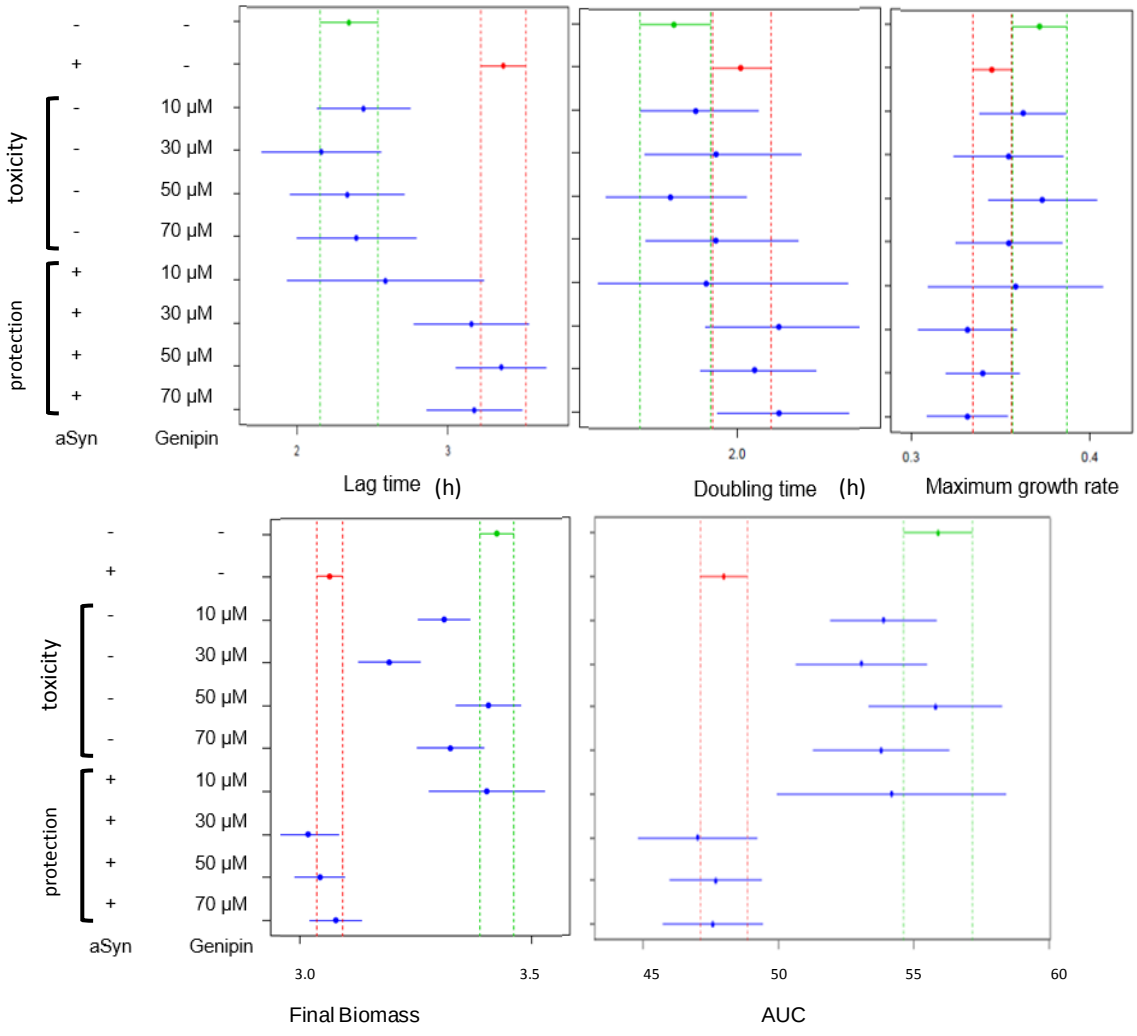

Figure III.1- Effect of genipin in cellular growth. (A) Growth curves of W303-1A_UT strain (green), aSyn-GFP strain (red) and aSyn-GFP strain treated with genipin (blue). The cultures were diluted in SC galactose medium and incubated for 24 h. (B) The 95% confidence interval for W303-1A_UT strain (green) and aSyn-GFP strain (red), for the growth parameters lag time, doubling time, maximum growth rate, final biomass and area under the curve were calculated using the "R" script. (C) The protection factor was calculated based on equation in page 14, -- in table indicates values lower than 0.

3.2. Role of genipin on aSyn inclusions

To assess the effect of genipin on the formation of aSyn-GFP inclusions, cells were induced 6 h in SC-galactose supplemented or not with 10 µM genipin. aSyn was shown to form intracellular inclusions in control cells, with low fluorescence signals at the plasma membrane, in agreement with data reported in the literature (51). By monitoring GFP fluorescence in cells treated with genipin it was observed a reduction in the formation of aSyn intracellular inclusions, with most of GFP fluorescence signals being detected at the plasma membrane (**Fig III.2A**). These data reinforce the notion that genipin may interfere with the formation of toxic intracellular inclusions.

A previous study evaluated the pre-treatment of aSyn-expressing cells with a (poly)phenol-enriched fraction (PEF) from *C. album* for 6 h in SC-raffinose medium followed by incubation with PEFs in SC-galactose medium (aSyn ON) for 12 h. The results showed that *C. album* PEF reduced the percentage of cells displaying aSyn-GFP inclusions (59). Here, the addition of genipin concomitantly with the induction of aSyn-GFP expression for 6 h, promoted the recovery of cellular growth. Thus, it was next assessed if this condition also triggers a decrease of the number of cells bearing aSyn-GFP inclusions. Indeed, under this condition the number of cells containing aSyn-GFP inclusions was dramatically reduced to 20%-30% as compared to the untreated aSyn strain (50%-70%) (**Fig III.2A,** right panel). These data suggest that genipin may be the compound conferring the protective activity of *C. album* PEF. Moreover, this effect was independent of aSyn-GFP protein levels since cells exposed or not to 10 µM genipin displayed similar aSyn-GFP levels (**Fig III.2B**)

The effect of genipin on the size of aSyn-GFP-containing inclusions was next evaluated by filter trap assays. This methodology allows the detection of large protein aggregates that are trapped on the acetate cellulose membrane. As shown in **Fig III.2C**, untreated cells displayed bigger aSyn-GFP signals in comparison with treated cells, indicating that genipin had the ability to decrease the size of aSyn-GFP inclusions. It should be noted, however, that the relation between size and toxicity of oligomeric aSyn-GFP species remains questionable and the process of amyloid formation is irreversible (17,85).

Previous *in vitro* studies have shown that other terpenoids inhibit aSyn fibrilization and toxicity, although only in high concentrations (>80 µM) (86). Genipin was revealed to be a more efficient compound in overcoming aSyn toxicity, since it improves cellular growth at very low concentrations (10 µM). It was also reported that genipin and geniposide prevent Ab_{25-35} toxicity, associated with Alzheimer's disease (68), strengthening the potential exploitation of this compound in the context of neurodegenerative disorders.

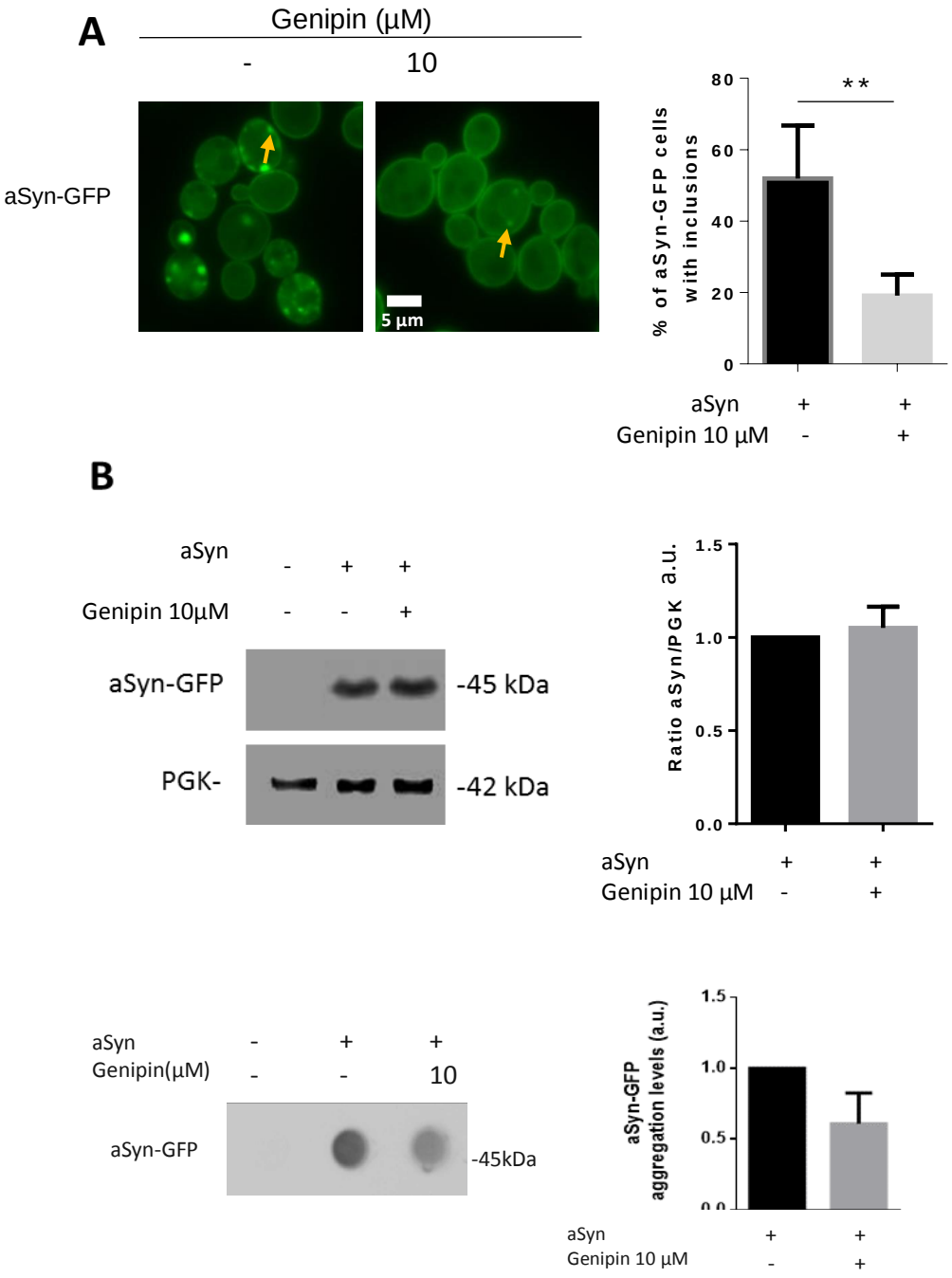

Figure III.2- Role of genipin on aSyn aggregation. (A) Cells induced in SC-galactose medium were incubated or not with genipin for 6 h and the number of cells displaying aSyn-GFP inclusions was assessed (right panel). (B) aSyn-GFP levels in cells subjected or not to genipin. The aSyn-GFP signals were quantified by densitometry. PGK was used as loading control (right panel). (C) The effect of genipin on the size of aggregates as evaluated by filter trap assays. The values represent the mean ± SD of at least three biological replicates, **p<0.01, unpaired t test with Welch's correction.

3.3. Effect of corilagin on the growth of FUS strain

The yeast model of FUS aggregation and toxicity was used to evaluate the ability of corilagin to modulate FUS proteotoxicity. Cell growth was monitored for 24 h in SC-glucose (control condition – FUS OFF) and SC-galactose (FUS ON) media supplemented or not with corilagin to a final concentration of 10, 30, 50, 70 µM. The 10 and 70 µM were the concentrations showed to be the less toxic for the W303-1B_H empty strain as assessed by the AUC values (**Fig.III.3B**).

As shown in **Fig. III.3A**, FUS expression led to a dramatic reduction of cellular growth in comparison with the W303-1B_H empty strain and the treatment with 70 µM corilagin partially restored cellular growth. Extraction of the growth parameters using the "R" script indicated that treatment with 70 µM corilagin had an impact on almost all the parameters studied. From the analysis of the growth parameters it is possible to conclude that FUS expression had a minor influence on the lag time of the cultures **Fig. III.3B**. The high toxicity of this protein seems to be related to the reduction of the maximum growth rate, which is associated with the reduction of the doubling time and consequently the final biomass. The treatment with 70 µM corilagin impacts on the maximum growth rate of the cultures, increasing the doubling time and final biomass in comparison with the untreated condition (**Fig. III.3B**) and leading to a protection factor of around 26.4% (**Fig. III.3C**).

The concomitant addition of corilagin to cultures with induction of FUS expression, suggest that corilagin may also interfere into a quick recover of cellular growth after induction of FUS expression and formation of intracellular aggregates.

A

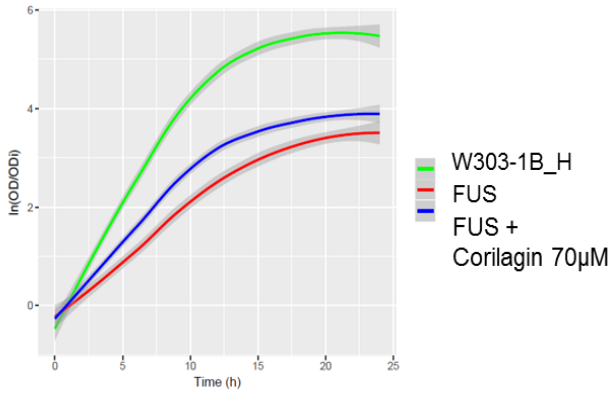

C

Condition : Corilagin	Protection factor %	P_Lower bound	P_Upper bound
10 µM	22.5	5.5	36.1
30 µM	--	--	3.5
50 µM	--	--	11.1
70 µM	26.4	12.6	37.5

B

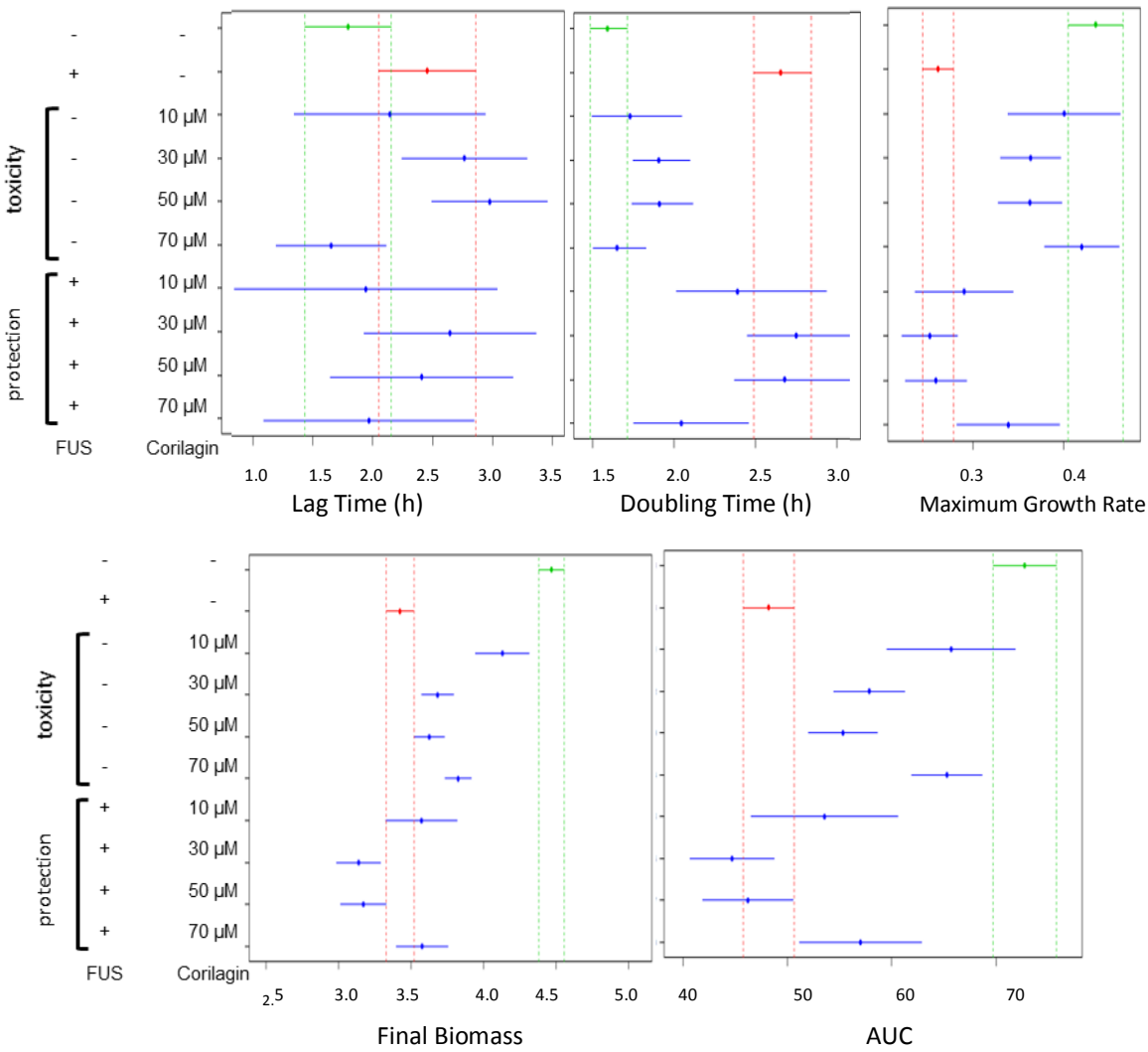

Figure III.3- Effect of corilagin in cellular growth (A) Growth curves of W303-1A_H (green) and FUS (red) strain incubated with corilagin (blue). The cultures were diluted in SC galactose medium and incubated for 24 h (B) The 95% confidence interval for W303-1A_H (green) and FUS strain (red), for the growth parameters lag time, doubling time, maximum growth rate, final biomass and AUC, were calculated using the "R" script (C) The protection factor was calculated based on equation in page 14 **--** on table indicates values lower than 0.

3.4. Role of corilagin in the superoxide radical levels of FUS strain

Superoxide radical levels were evaluated as an indicator of oxidative stress, since this state is linked to the aggregation of misfolded proteins and FUS-induced toxicity (20,50). Superoxide was analyzed by flow cytometry using dihydroethidium (DHE) (**Supplementary data VI.1A**) and the results indicate higher superoxide signals in the FUS strain compared to W303-1B_H empty strain. However, no significant differences were observed between untreated and corilagin-treated cells expressing FUS (**Fig.III.4A**). Thus, the detected improvement of cellular growth mediated by corilagin cannot be attributed to the regulation of superoxide levels. Next, cell viability was evaluated using propidium iodide (PI) (**Supplementary data VI.1B**)**.** The data showed a higher percentage of PI positive cells in FUS strain compared to the W303-1B_H but no significant differences were observed between untreated and corilagin-treated cells expressing FUS (**Fig.III.4B**).

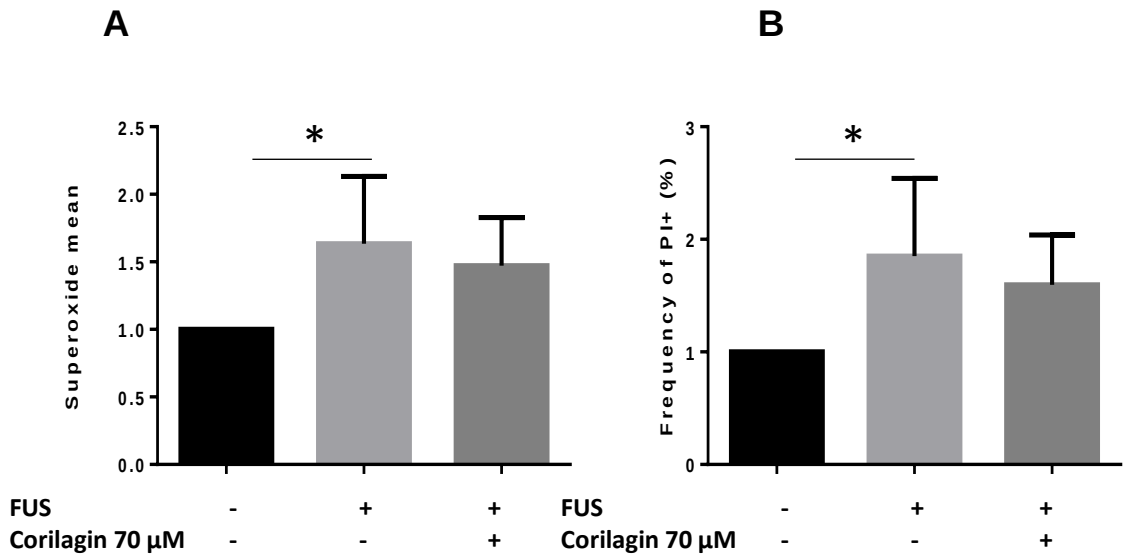

Figure III.4- Corilagin does not affect superoxide radical levels or cell viability, after 6 h of incubation in SC-galactose medium with 70 µM corilagin (A) Superoxide radical mean assessed by FCM using DHE probe (B) Frequency of PI-positive cells. Values represent the mean ± SD of at least three independent experiments * P<0.05; One way ANOVA with Kruskal-Wallis.

3.5. Subcellular localization and FUS inclusions

Previous data indicate that treatment with extracts of *R. genevieri,* from which corilagin was identified, trigger a reduction of FUS levels in comparison with the untreated condition, when protein extracts are prepared using a mild extraction condition (tris-buffered saline (TBS) plus ultrasounds) (**Fig. III.5A**, upper panel). The fact that FUS levels remain unaltered in protein extracts prepared under harsh conditions (using TCA, acetone, and a combination of detergents) (**Fig. III.5A**, lower panel), suggests that the *R. genevieri* extract possibly triggers the sequestering of FUS to a cellular compartment inaccessible to the TBS extraction procedure. If corilagin is the bioactive compound of the *R. genevieri* extract, it is plausible to consider that corilagin will induce a similar effect. This hypothesis was tested by preparing TBS and TCA protein extracts from FUS-expressing cells subjected or not to a treatment with 70 µM corilagin for 6 h in SC-galactose media. As shown in **Fig. III.5B**, corilagin mediated a similar reduction of FUS levels in protein extracts prepared with TBS whereas its levels remained unaltered in the TCA-prepared extracts, strongly supporting corilagin as the bioactive compound of *R. genevieri*.

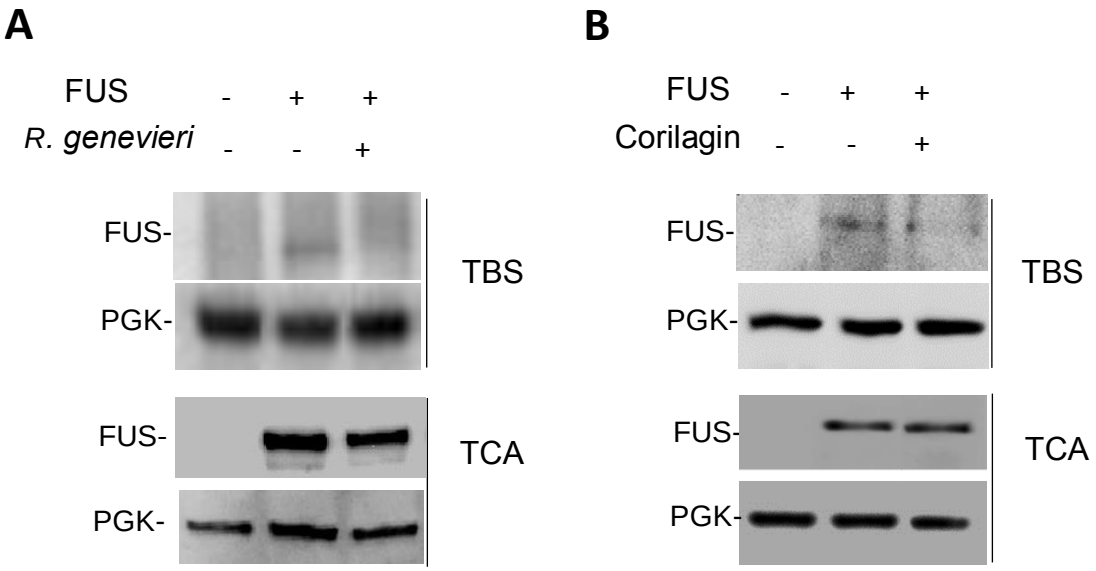

Figure III.5-FUS expression levels of cells (PGK as loading control), assessed by western blot. (A) Cells subjected to the extract, 250 µg GAE.mL^{-1} was the higher non-toxic concentration tolerated by cells as defined in the cytotoxicity assays (B) Cells subjected to the compound, 70 µM of corilagin. Illustrative images of at least three biological replicates.

These data led to the next questions: What is the intracellular localization of FUS? and how does corilagin affect FUS intracellular distribution?

It is well known that unfolded or misfolded proteins can be accumulated in the lumen of the endoplasmic reticulum (ER), generating a condition called ER stress (87). To evaluate if this

compartment was involved in corilagin-mediated protection, co-localization studies were performed using a GFP-FUS fusion and Sec13 fused to RFP. Sec13 is a subunit of the COPII vesicle coat required for ER-to-Golgi transport, being therefore used as a marker of ER (88). Since Sec13-RFP is encoded as an integrated copy in the genome of BY4741 yeast strain, the non-toxic range of corilagin in the BY4741 and BY4741_Sec13-RFP strains was first evaluated by growth assays. The protective profile of the compound was also tested in the BY4741_GFP-FUS and BY4741_SEC13-RFP_GFP-FUS strains. Unexpectedly, corilagin did not protect those strains (**Supplementary data VI.2**) even using higher corilagin concentrations (100 µM, which was not toxic in the BY4741 background). This observation indicates that the different genetic backgrounds of the strains had a major influence on the observed phenotype, and therefore further experiments with the BY4741_Sec13-RFP_GFP-FUS strain were not performed.

The vacuole, the analogous of the mammalian lysosome, is the main cellular site of protein turnover and plays a central role for degradation of proteins (89). In *S. cerevisiae* the Zrc1 protein has been implicated in zinc transport from cytosol to vacuole for storage, serving as an efficient marker of yeast vacuole.

To investigate the possible accumulation of FUS in the vacuole, the same approach as in the ER colocalization experiments was used (90). The non-toxic range of corilagin in the BY4742 and the BY4742_Zrc1-mCherry, empty strains were first evaluated by growth assays. The protective profile of the non-toxic concentrations of corilagin in BY4742_GFP-FUS and in BY4742_Zrc1-mCherry_GFP-FUS was also tested (**Supplementary data VI.3 and Fig.III.6,** respectively). Extraction of growth parameters indicated that treatment of the BY4742_Zrc1-mCherry_GFP-FUS strain with 100 µM corilagin enhanced the doubling time, maximum growth rate and AUC, leading to a protection factor of around 27% **Fig.III.6B** and **Fig.III.6C**.

The changing of the strain did not affect the compound effect. However, an increase in concentration (100 µM) demonstrated an improvement in growth parameters, which was expected due to the higher drug resistance of BY4742 strain compared to W303_1A (91).

A

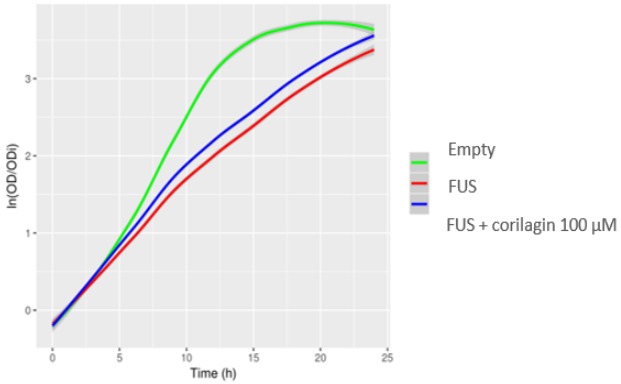

C

Condition	Protection factor %	P_LBound	P_UBound
Corilagin 100µM	27	7.6	40.7

B

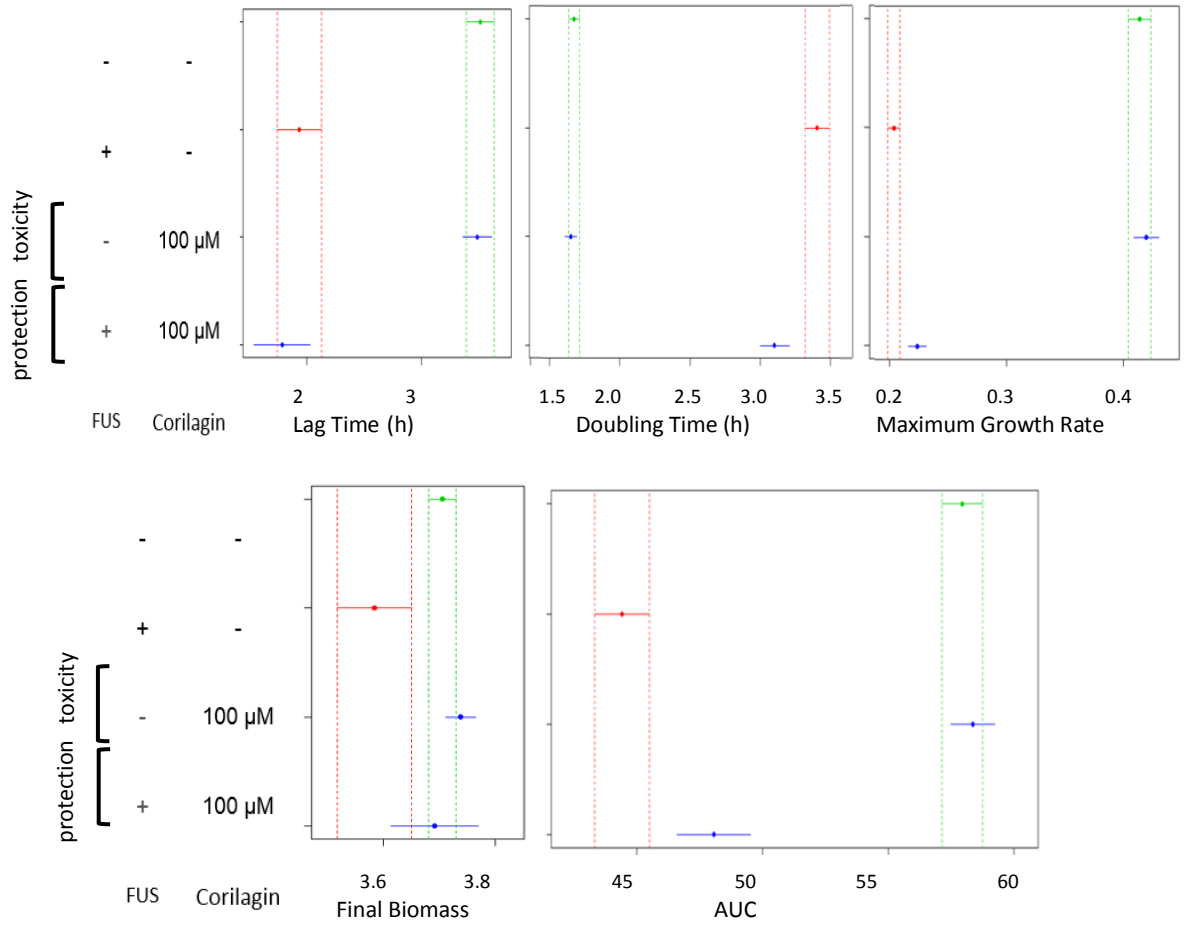

Figure III.6- Effect of corilagin in cellular growth (A) Growth curves of BY4742_Zrc1-mCherry (green), BY4742_Zrc1-mCherry_GFP-FUS (red) strain incubated with 100 µm corilagin (blue). The cultures were diluted in SC-URA galactose medium for 24 h (B) The 95% confidence interval for BY4742_Zrc1-mCherry (green), BY4742_Zrc1-mCherry_GFP-FUS (red), the growth parameters lag time, doubling time, maximum growth rate, final biomass and AUC, were calculated using the "R" script (C) The protection factor was based on equation in page 14.

Once the corilagin protection was established, it was next evaluated whether FUS associates with the vacuole in yeast. To address this issue, BY4742 cells expressing Zrc1-mCherry_GFP-FUS were treated with 100 µM corilagin for 6 h in SC-galactose medium and fluorescence microscopy was performed. The overlap of mCherry and GFP fluorescence was evaluated by the quantification of cells with yellow signals resulting from the merge of the red and green channels **Fig.III.7B** (92). Indeed, under treatment with corilagin a huge accumulation of FUS was detected in the vacuole (20-25%) as compared to untreated cells (3-5%) **Fig.III.7C**. This evidence led us to hypothesize that the FUS inclusions were mobilized to the vacuole. Cells expressing only ZRC1-mCherry and an empty vector were processed in parallel (**Fig.III.7A**). By quantifying the number of cells with FUS inclusions it was demonstrated that are no differences between control cells and treated cells (**Fig.III.8**). Therefore, corilagin protection was mediated by sequester of protein aggregates to vacuole.

Aggregate-prone proteins are commonly degraded by autophagy and lastly delivered to the lysosome (93). The link between mutant FUS, cytoplasmic aggregates and the impact of autophagy on FUS has been already described, as well as autophagy activation as a therapeutic approach for FUS mutation-associated with ALS (94). In this study, it was shown that corilagin induces the sequestering of FUS inclusions into vacuoles. This phenolic compound may represent an important therapeutic strategy for delaying the progression of ALS associated with FUS mutations.

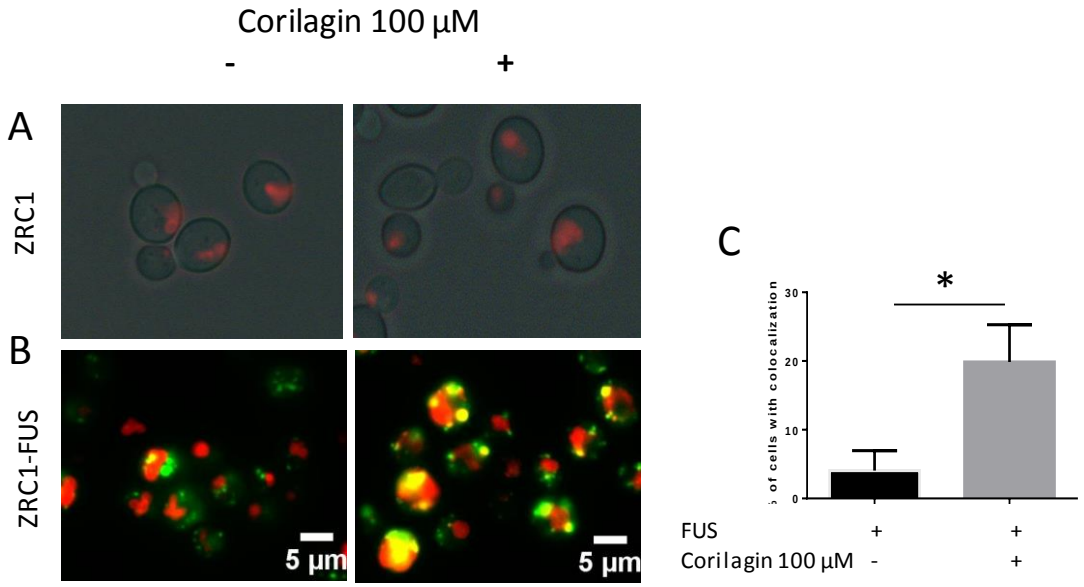

Figure III.7- Cells expressing Zrc1-mCherry and GFP-FUS were grown in SC-URA galactose for 6 h. (A) Empty cells (B) GFP-FUS inclusions colocalize with Zrc1-mCherry in vacuole (C) Percentage of cells with colocalization. The values represent the mean ± SD of at least three biological replicates, *p<0.05; Unpaired t test with Welch's correction.

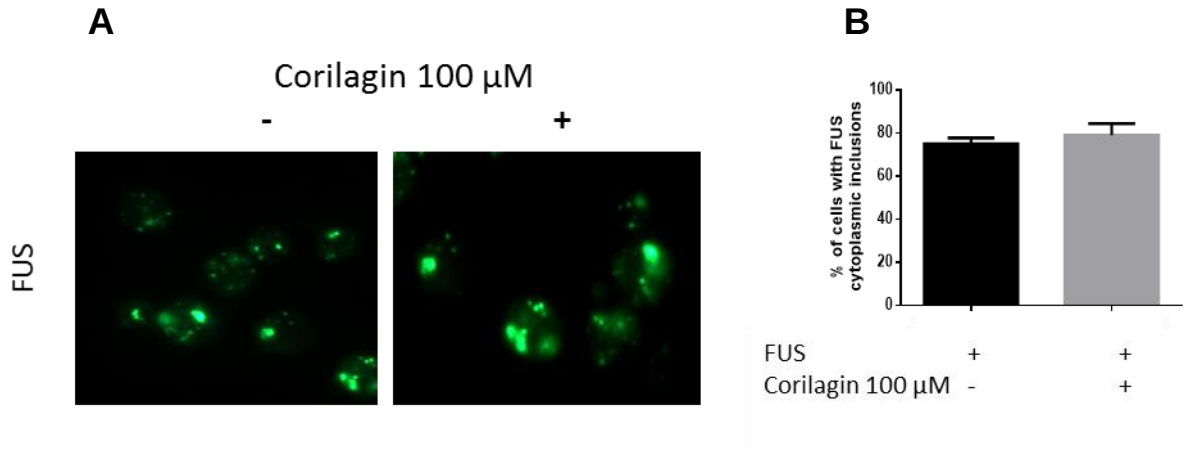

Figure III.8 – Corilagin effect on FUS aggregation (A) Intracellular localization of FUS without and with treatment. Cell cultures grown in SC-URA galactose for 6 h (B) Percentage of cells containing FUS inclusions. The values represent the mean ± SD of at least three biological replicates.

4. Conclusions and future perspectives

Parkinson's disease and amyotrophic lateral sclerosis are incurable disorders affecting millions of people worldwide. There is an urgent demand for the development of novel therapeutic strategies improving the quality of life of patients and delaying disease progression. Oxidative stress and protein misfolding and aggregation have been long implicated in neurodegenerative diseases. Therefore, the underlying molecular pathways constitute interesting targets to be scrutinized. On the other hand, the search for potential phytochemicals as protective agents against the pathological processes of these diseases has generated new expectations for improvements in health.

In this study, phytochemicals from *Corema album* leaf and *Rubus genevieri* fruit, pointed as the potential bioactive compounds conferring the protective activity of the extracts for Parkinson's disease and amyotrophic lateral sclerosis, respectively, were investigated using *Saccharomyces cerevisiae* as a model organism. The objective was to validate their bioactivity and characterize their function towards particular pathological processes of these diseases.

The data showed that genipin, the compound isolated from *Corema album*, confers protection to yeast cells expressing aSyn by similar mechanisms to those of (poly)phenol-enriched extract. Both PEF and genipin improve the cellular growth impaired by the expression of aSyn in a mechanism that seems to be related to the modulation of the formation of aSyn aggregates. The modulation of aSyn is of extreme importance as a therapeutic target in Parkinson's disease and other synucleopathies. The *Corema album* leaf PEF was also shown to be a potent agent against oxidative stress, and it also promotes aSyn-GFP clearance (59). It remains to be elucidated whether genipin also modulates these processes.

The data obtained in this study also validated corilagin as a compound conferring the protective activity of *Rubus genevieri* fruit for Amyotrophic Lateral Sclerosis. Corilagin recover cellular growth of yeast cells expressing FUS in a similar manner of *Rubus genevieri* fruit PEF. In addition, both PEF and corilagin seems to trigger the sequestering of FUS into the vacuole, possibly as mechanism to get rid of toxic aggregates from the cytosol. Autophagy has been described as a potent therapeutic approach for amyotrophic lateral sclerosis (94). It remains to elucidate the involvement of autophagy in this process.

There is still much to learn about the molecular targets of these phytochemicals, therefore, efforts should be done to further understand their mode of action as well as to validate the results in mammalian models.

The main concern of phytochemicals is their low bioavailability, which can be overcome using encapsulation technologies.

These results are promising, although preliminary and a deeper investigation may open new venues for the harnessing of these compounds as lead molecules for Parkinson's disease and amyotrophic lateral sclerosis therapeutics.

CHAPTER V- BIBLIOGRAPHY

1. http://www.pdf.org/parkinson_statistics [Internet]. 2017. Available from: http://www.pdf.org/parkinson_statistics
2. Baker M, Gershanik O. Parkinson's disease. In: Neurological Disorders public health challenges. 2006.
3. Traynor BJ, Arthur KC, Calvo A, Price TR, Geiger JT, Chio A. Projected increase in amyotrophic lateral sclerosis from 2015 to 2040. Nat Commun. 2016;7:1–6.
4. Kumar D. The Father of Neurology. Clin Med Res. 2011;9(1):46–9.
5. Kim GH, Kim JE, Rhie SJ, Yoon S. The Role of Oxidative Stress in Neurodegenerative Diseases. 2015;24(4):325–40.
6. Ursini F, Maiorino M, Jay H. Redox Biology Redox homeostasis : The Golden Mean of healthy living. Redox Biol [Internet]. Elsevier; 2016;8:205–15. Available from: http://dx.doi.org/10.1016/j.redox.2016.01.010
7. Sies H, Jones D. Oxidative stress. In: Encyclopedia of Stress. G Fink. Amsterdam: Elsevier. 2nd ed.; 2007. p. 45–8.
8. Lushchak VI. Chemico-Biological Interactions Free radicals , reactive oxygen species , oxidative stress and its classification. Chem Biol Interact [Internet]. Elsevier Ireland Ltd; 2014;(October). Available from: http://dx.doi.org/10.1016/j.cbi.2014.10.016
9. Sies H, Berndt C, Jones DP. Oxidative Stress. Annu Rev Biochem. 2017;86(April):25.1-25-34.
10. Tabart J, Kevers C, Pincemail J, Defraigne J, Dommes J. Comparative antioxidant capacities of phenolic compounds measured by various tests. Food Chem [Internet]. Elsevier Ltd; 2009;113(4):1226–33. Available from: http://dx.doi.org/10.1016/j.foodchem.2008.08.013
11. Rahal A, Kumar A, Singh V, Yadav B, Tiwari R, Chakraborty S, et al. Oxidative Stress , Prooxidants , and Antioxidants : The Interplay. Biomed Res Int. 2014;2014:19 pages.
12. Niedzielska E, Smaga I, Gawlik M, Moniczewski A. Oxidative Stress in Neurodegenerative Diseases. 2015;
13. Cordeiro RM. Biochimica et Biophysica Acta Reactive oxygen species at phospholipid bilayers : Distribution , mobility and permeation. BBA - Biomembr [Internet]. Elsevier B.V.; 2014;1838(1):438–44. Available from: http://dx.doi.org/10.1016/j.bbamem.2013.09.016
14. Costa J, Carvalho M De. Emerging molecular biomarker targets for amyotrophic lateral sclerosis. Clin Chim Acta. Elsevier B.V.; 2016;
15. Frijhoff J, Winyard PG, Zarkovic N, Davies SS, Stocker R, Cheng D, et al. Clinical Relevance of Biomarkers of Oxidative Stress 1. Antioxidants Redox Signal. 2015;23(14):1144–70.
16. Ross C, Poirier M. What is the role of protein aggregation in neurodegeneration ? Nat Rev Cell Biol. 2005;6(November):891–8.
17. Knowles TPJ, Vendruscolo M, Dobson CM. The amyloid state and its association with protein misfolding diseases. Nat Publ Gr [Internet]. Nature Publishing Group; 2014;15(6):384–96. Available from: http://dx.doi.org/10.1038/nrm3810
18. Bucciantini M, Giannoni E, Chiti F, Baroni F, Formigli L. Inherent toxicity of aggregates implies a common mechanism for protein misfolding diseases. Nature. 2002;416:507–11.
19. Jucker M, Walker LC. Self-propagation of pathogenic protein aggregates in neurodegenerative diseases. Nature [Internet]. Nature Publishing Group; 2013;501(7465):45–51. Available from: http://dx.doi.org/10.1038/nature12481
20. Sze CI, Kuo YM, Hsu LJ, Fu TF, Chiang MF, Chang JY, et al. A cascade of protein aggregation bombards mitochondria for neurodegeneration and apoptosis under WWOX deficiency. Cell death Dis. 2015;5–6.
21. Parkinson J. An Essay on the Shaking Palsy. J Neuropsychiatry Clin Neurosci. 2002;14(2):223–36.
22. Jenner P, Morris HR, Robbins TW, Goedert M, Hardy J. Europe PMC Funders Group Parkinson ' s Disease – the Debate on the Clinical Phenomenology , Aetiology , Pathology and Pathogenesis. J Park Dis. 2014;3(1):1–11.
23. Tenreiro S, Reimão-Pinto MM, Antas P, Rino J, Wawrzycka D, Macedo D, et al. Phosphorylation Modulates Clearance of Alpha-Synuclein Inclusions in a Yeast Model of Parkinson's Disease. PLoS Genet. 2014;10(5).
24. Xu W, Tan L, Yu J. Neurobiology of Aging The link between the SNCA gene and parkinsonism. Neurobiol Aging [Internet]. Elsevier Inc; 2014;1–14. Available from: http://dx.doi.org/10.1016/j.neurobiolaging.2014.10.042
25. Pasanen P, Myllykangas L, Siitonen M, Raunio A, Kaakkola S, Lyytinen J, et al. A novel

a-synuclein mutation A53E associated with atypical multiple system atrophy and Parkinson's disease-type pathology. Neurobiol Aging [Internet]. Elsevier Ltd; 2014;1–5. Available from: http://dx.doi.org/10.1016/j.neurobiolaging.2014.03.024
26. Bendor J, Logan T, Edwards RH. The Function of α -Synuclein. Neuron. 2014;79(6):1–43.
27. Su LJ, Auluck PK, Outeiro TF, Yeger-lotem E, Kritzer JA, Tardiff DF, et al. Compounds from an unbiased chemical screen reverse both ER-to-Golgi trafficking defects and mitochondrial dysfunction in Parkinson's disease models. Dis Model Mech. 2010;208:194–208.
28. Sharma N, Brandis KA, Herrera SK, Johnson BE, Vaidya T, Shrestha R, et al. α -Synuclein Budding Yeast Model. 2006;28:161–78.
29. Villar-piqué A, Lopes T, Sant R, Mónika É, Fonseca-ornelas L. Environmental and genetic factors support the dissociation between α -synuclein aggregation and toxicity.
30. Winner B, Jappelli R, Maji SK, Desplats PA, Boyer L, Aigner S. In vivo demonstration that α -synuclein oligomers are toxic. Proc Natl Acad Sci U S A. 2011;108(10):4194–9.
31. Al-chalabi A, Berg LH Van Den, Veldink J. Gene discovery in amyotrophic. Nat Publ Gr [Internet]. Nature Publishing Group; 2016;13(2):96–104. Available from: http://dx.doi.org/10.1038/nrneurol.2016.182
32. Goldstein LH, Abrahams S. Changes in cognition and behaviour in amyotrophic lateral sclerosis : nature of impairment and implications for assessment. Lancet Neurol [Internet]. Elsevier Ltd; 2013;12(4):368–80. Available from: http://dx.doi.org/10.1016/S1474-4422(13)70026-7
33. Blokhuis AM, Groen EJN, Koppers M, Van Den Berg LH, Pasterkamp RJ. Protein aggregation in amyotrophic lateral sclerosis. Acta Neuropathol. 2013;125(6):777–94.
34. Kaur SJ, Mckeown SR, Rashid S. Mutant SOD1 mediated pathogenesis of Amyotrophic Lateral Sclerosis. Gene. Elsevier B.V.; 2016;577(2):109–18.
35. Sreedharan J. TDP-43 Mutations in Familial and Sporadic Amyotrophic Lateral Sclerosis. Science (80-). 2013;1668(2008).
36. Sedlmeier R, Meyer T. Point mutations of the p150 subunit of dynactin (DCTN1) gene in ALS. Neurology. 2004;
37. Zou Z, Liu M, Li X, Cui L. Degeneration Mutations in FUS are the most frequent genetic cause in juvenile sporadic ALS patients of Chinese origin. 2016;8421(March).
38. Hübers A, Just W, Rosenbohm A, Müller K, Marroquin N, Goebel I, et al. Neurobiology of Aging De novo FUS mutations are the most frequent genetic cause in early-onset German ALS patients. Neurobiol Aging [Internet]. Elsevier Inc; 2015;36(11):3117.e1-3117.e6. Available from: http://dx.doi.org/10.1016/j.neurobiolaging.2015.08.005
39. Vance C, Rogelj B, Hortobágyi T, De Vos KJ, Nishimura AL, Sreedharan J, et al. Mutations in FUS, an RNA Processing Protein, Cause Familial Amyotrophic Lateral Sclerosis Type 6. Science (80-). 2009;323(February):1208–11.
40. Hewitt C, Kirby J, Highley JR, Hartley JA, Hibberd R, Hollinger HC, et al. Novel FUS/TLS Mutations and Pathology in Familial and Sporadic Amyotrophic Lateral Sclerosis. Arch Neurol. 2015;67(4):455–61.
41. Eneroth M, Mandahl N, Heim S, Rydholm A, Alberts KA. Localization of the Cromosomal Breakpoints of the t(12;16) in Liposarcoma to Subbands. Cancer Genet Cytogenet. 1990;107:101–7.
42. Hosler BA, Cortelli P, Jong PJ De, Yoshinaga Y, Haines JL. Mutations in the FUS/TLS Gene on Chromosome 16 Cause Familial Amyotrophic Lateral Sclerosis. Science (80-). 2009;547(April).
43. Sharma A, Lyashchenko AK, Lu L, Nasrabady SE, Elmaleh M, Mendelsohn M, et al. ALS-associated mutant FUS induces selective motor neuron degeneration through toxic gain of function. Nat Commun [Internet]. Nature Publishing Group; 2016;7:1–14. Available from: http://dx.doi.org/10.1038/ncomms10465
44. Figley MD, Gitler AD. Yeast genetic screen reveals novel therapeutic strategy for ALS. Rare Dis (Austin, Tex). 2013;1:e24420.
45. Scekic-zahirovic J, Sendscheid O, Oussini H El, Jambeau M, Sun Y, Mersmann S, et al. Toxic gain of function from mutant FUS protein is crucial to trigger cell autonomous motor neuron loss. EMBO J. 2016;1–21.
46. Tenreiro S, Outeiro TF. Simple is good : yeast models of neurodegeneration. Fed Eur Microbiol Soc. 2010;10:970–9.
47. Menezes R, Tenreiro S, Macedo D, Santos CN, Outeiro TF. From the baker to the bedside: yeast models of Parkinson's disease. Microb Cell. 2015;2(8):262–79.

48. Goffeau A, Barrell BG, Bussey H, Davis RW, Dujon B, Feldmann H, et al. Life with 6000 Genes conveniently among the different interna- Old Questions and New Answers The genome . At the beginning of the se- of its more complex relatives in the eukary- cerevisiae has been completely sequenced Schizosaccharomyces pombe indicate. Science (80-). 1996;274(October):546–67.
49. Giaever G, Chu A, Dow S, Lucau-danila A, Anderson K, Arkin AP, et al. Functional profiling of the Saccharomyces cerevisiae genome. Nat Publ Gr. 2002;418:1–5.
50. Ju S, Tardiff DF, Han H, Divya K, Zhong Q, Maquat LE, et al. A Yeast Model of FUS / TLS-Dependent Cytotoxicity. PLOS Biol. 2011;9(4):17.
51. Outeiro TF, Lindquist S. Yeast Cells Provide Insight into Alpha-Synuclein Biology and Pathobiology. 2003;302(December):1772–6.
52. Corti O, Lesage S, Brice A. What genetics tells us about the causes and mechanisms of Parkinson's disease. Physiol Rev. 2011;91:1161–218.
53. Kasote DM, Katyare SS, Hegde M V, Bae H. Significance of Antioxidant Potential of Plants and its Relevance to Therapeutic Applications. Int J Biol Sci. 2015;11:982–91.
54. Huang L, Su X, Federoff HJ. Single-Chain Fragment Variable Passive Immunotherapies for Neurodegenerative Diseases. Int J Mol Sci. 2013;14:19109–27.
55. Stefani M, Rigacci S. Beneficial properties of natural phenols : Highlight on protection against pathological conditions associated with amyloid aggregation. Biofactors. 2014;40(5):1–12.
56. Hamaguchi T, Ono K. Phenolic Compounds Prevent Alzheimer's Pathology through Different Effects on the Amyloid-b Aggregation Pathway. Am J Pathalogy. 2009;175(6):2557–65.
57. Elbling L, Weiss R, Teufelhofer O, Uhl M, Knasmueller S, Schulte-hermann R, et al. Green tea extract and (–) -epigallocatechin-3-gallate , the major tea catechin , exert oxidant but lack antioxidant activities. FASEB J. 2005;19:807–9.
58. Venkatesan R, Ji E, Kim SY. Phytochemicals That Regulate Neurodegenerative Disease by Targeting Neurotrophins : A Comprehensive Review. Biomed Res Int. 2015;2015:22.
59. Macedo D, Tavares L, McDougall GJ, Vicente Miranda H, Stewart D, Ferreira RB, et al. (Poly)phenols protect from a-synuclein toxicity by reducing oxidative stress and promoting autophagy. Hum Mol Genet. 2014;24(6):1717–32.
60. Dudnik A. BacHBerry: BACterial Hosts for production of Bioactive phenolics from bERRY fruits. Phytochemistry. 2017;
61. Li Y, Li L, Ho C. Therapeutic Potential of Genipin in Central Neurodegenerative Diseases. CNS Drugs. 2016;
62. Singh G, Vinod AKV. Catalytic properties , functional attributes and industrial applications of b -glucosidases. 3 Biotech. Springer Berlin Heidelberg; 2016;6(1):1–14.
63. Manickam B, Sreedharan R, Elumalai M. " Genipin " – The Natural Water Soluble Cross-linking Agent and Its Importance in the Modified Drug Delivery Systems : An Overview. Curr Drug Deliv. 2014;11:139–45.
64. Koo H, Seon Y, Kim H, Lee Y, Hong S, Kim S, et al. Antiinflammatory effects of genipin , an active principle of gardenia. Eur J Pharmacol. 2004;495:201–8.
65. Hughes RH, Silva VA, Ahmed I, Shreiber DI, Morrison B. Neuroprotection by genipin against reactive oxygen and reactive nitrogen species-mediated injury in organotypic hippocampal slice cultures. Brain Res [Internet]. Elsevier; 2014;1543:308–14. Available from: http://dx.doi.org/10.1016/j.brainres.2013.11.020
66. Salminena A, Lehtonenc M, Suuronen T, Kaarnirantada K, Huuskonen J. Terpenoids : natural inhibitors of NF- k B signaling with anti-inflammatory and anticancer potential. Cell Mol Life Sci. 2008;65:2979–99.
67. Oliver E, Luo D, Or TCT, Yang CLH, Lau ASY. Anti-Inflammatory Activity of Iridoid and Catechol Derivatives from Eucommia ulmoides Oliver. Am Chem Soc Chem Neurosci. 2014;5:855–66.
68. Yamazaki MY, Akura NS, Hiba KC. Prevention of the Neurotoxicity of the Amyloid b Protein by Genipin. Biol Pharm Bull. 2001;24(12):1454–5.
69. Gouras GK, Almeida CG, Takahashi RH. Intraneuronal AB accumulation and origin of plaques in Alzheimer's disease. Neurobiol Aging. 2005;26:1235–44.
70. Chen Y, Zhang Y, Li L. Neuroprotective effects of geniposide in the MPTP mouse model of Parkinson's disease. Eur J Pharmacol [Internet]. Elsevier; 2015;768:21–7. Available from: http://dx.doi.org/10.1016/j.ejphar.2015.09.029
71. Liu J, Yin F, Guo L, Zhang J, Zidichouski J. Molecular Mechanisms of Geniposide and

Genipin Against Alzheimer ' s Disease. In: Bioactive Nutraceuticals and Dietary Supplements in Neurological and Brain Disease [Internet]. Elsevier Inc.; 2015. p. 221–7. Available from: http://dx.doi.org/10.1016/B978-0-12-411462-3.00024-2

72. Koo H, Lim K, Jung H, Park E. Anti-inflammatory evaluation of gardenia extract , geniposide and genipin. 2006;103:496–500.
73. https://pubchem.ncbi.nlm.nih.gov/compound/442424.
74. Youn K, Lee S, Jeong W. Protective Role of Corilagin on Ab25–35-Induced Neurotoxicity: Suppression of NF-kB Signaling Pathway. J Med food. 2016;0(0):1–11.
75. Zhao L, Zhang S, Tao J, Pang R, Jin F. Preliminary exploration on anti-inflammatory mechanism of Corilagin (beta-1- O -galloyl-3 ,. 2008;1059–64.
76. Jin F, Cheng D, Tao J, Zhang S, Pang R, Guo Y, et al. Anti-inflammatory and anti-oxidative effects of corilagin in a rat model of acute cholestasis. BMC Gastroenterol. 2013;13(79):1–10.
77. Chen Y, Chen C. Neurochemistry International Corilagin prevents tert-butyl hydroperoxide-induced oxidative stress injury in cultured N9 murine microglia cells. Neurochem Int [Internet]. Elsevier B.V.; 2011;59(2):290–6. Available from: http://dx.doi.org/10.1016/j.neuint.2011.05.020
78. Cechinel V, Moreira J, Klein-ju LC. Anti-hyperalgesic activity of corilagin , a tannin isolated from Phyllanthus niruri L . (Euphorbiaceae). J Ethnopharmacol. 2013;146:318–23.
79. Thomas BJ, Rothstein R. Elevated Recombination Rates in Transcriptionally Active DNA. Cell. 1989;56:619–30.
80. Brachmann CB, Davies A, Cost GJ, Caputo E. Designer Deletion Strains derived from Saccharomyces cerevisiae S288C : a Useful set of Strains and Plasmids for PCR-mediated Gene Disruption and Other Applications. Yeast. 1998;132:115–32.
81. Huh W, Falvo J V, Gerke LC, Carroll AS, Howson RW, Weissman JS, et al. Global analysis of protein localization in budding yeast. Nat Publ Gr. 2003;425:686–91.
82. Miller-fleming L, Cheong H, Antas P, Klionsky DJ. Detection of Saccharomyces cerevisiae Atg13 by western blot. 2014;10(3):514–7.
83. Alberti S, Halfmann R, Lindquist S. Biochemical , Cell Biological , and Genetic Assays to Analyze Amyloid and Prion Aggregation in Yeast [Internet]. 2nd ed. Guide to Yeast Genetics: Functional Genomics, Proteomics, and Other Systems Analysis. Elsevier Inc; 709-734 p. Available from: http://dx.doi.org/10.1016/S0076-6879(10)70030-6
84. Chang E, Kuret J. Detection and Quantification of Tau Aggregation Using a Membrane Filter Assay. Anal Biochem. 2009;373(2):330–6.
85. Siddiqi M, Alam P, Chaturved S, Shahein YE. Mechanisms of protein aggregation and inhibition. Front Biosci. 2017;9.
86. Masuda M, Suzuki N, Taniguchi S, Oikawa T, Nonaka T. Small Molecule Inhibitors of R -Synuclein Filament Assembly †. 2006;6085–94.
87. Oslowski CM, Urano F. Measuring ER stress and the unfolded protein response using mammalian tissue culture system. Methods Enzymol. 2013;490:71–90.
88. Lemus L, Ribas JL, Lemus L, Ribas JL, Sikorska N, Goder V. An ER-Localized SNARE Protein Is Exported in Specific COPII Vesicles for Autophagosome Article An ER-Localized SNARE Protein Is Exported in Specific COPII Vesicles for Autophagosome Biogenesis. CellReports [Internet]. The Authors; 2016;14(7):1710–22. Available from: http://dx.doi.org/10.1016/j.celrep.2016.01.047
89. Teter SA, Klionsky DJ. Transport of proteins to the yeast vacuole: autophagy, cytoplasm-to-vacuole targeting, and role of the vacuole in degradation. Cell Dev Biol. 2000;11:173–9.
90. Macdiarmid CW, Gaither LA, Eide D. Zinc transporters that regulate vacuolar zinc storage in Saccharomyces cerevisiae. EMBO J. 2000;19(12):2845–55.
91. Stefanini I, Trabocchi A, Marchi E, Guarna A, Cavalieri D. A Systems Biology Approach to Dissection of the Effects of Small Bicyclic Peptidomimetics on a Panel of Saccharomyces cerevisiae Mutants. J Biol Chem VOL. 2010;285(30):23477–85.
92. Klionsky DJ, Abdelmohsen K, Abe A, Abedin J, Abeliovich H, Bartolom A, et al. Guidelines for the use and interpretation of assays for monitoring autophagy (3rd edition). 2016;12(1):1–222.
93. Nixon RA. review The role of autophagy in neurodegenerative disease. Nat Med [Internet]. Nature Publishing Group; 2013;19(8):983–97. Available from: http://dx.doi.org/10.1038/nm.3232
94. Ryu H, Jun M, Min K, Jang D, Lee Y, Kyu H, et al. Neurobiology of Aging Autophagy

regulates amyotrophic lateral sclerosis-linked fused in sarcoma-positive stress granules in neurons. Neurobiol Aging [Internet]. Elsevier Ltd; 2014;35(12):2822–31. Available from: http://dx.doi.org/10.1016/j.neurobiolaging.2014.07.026

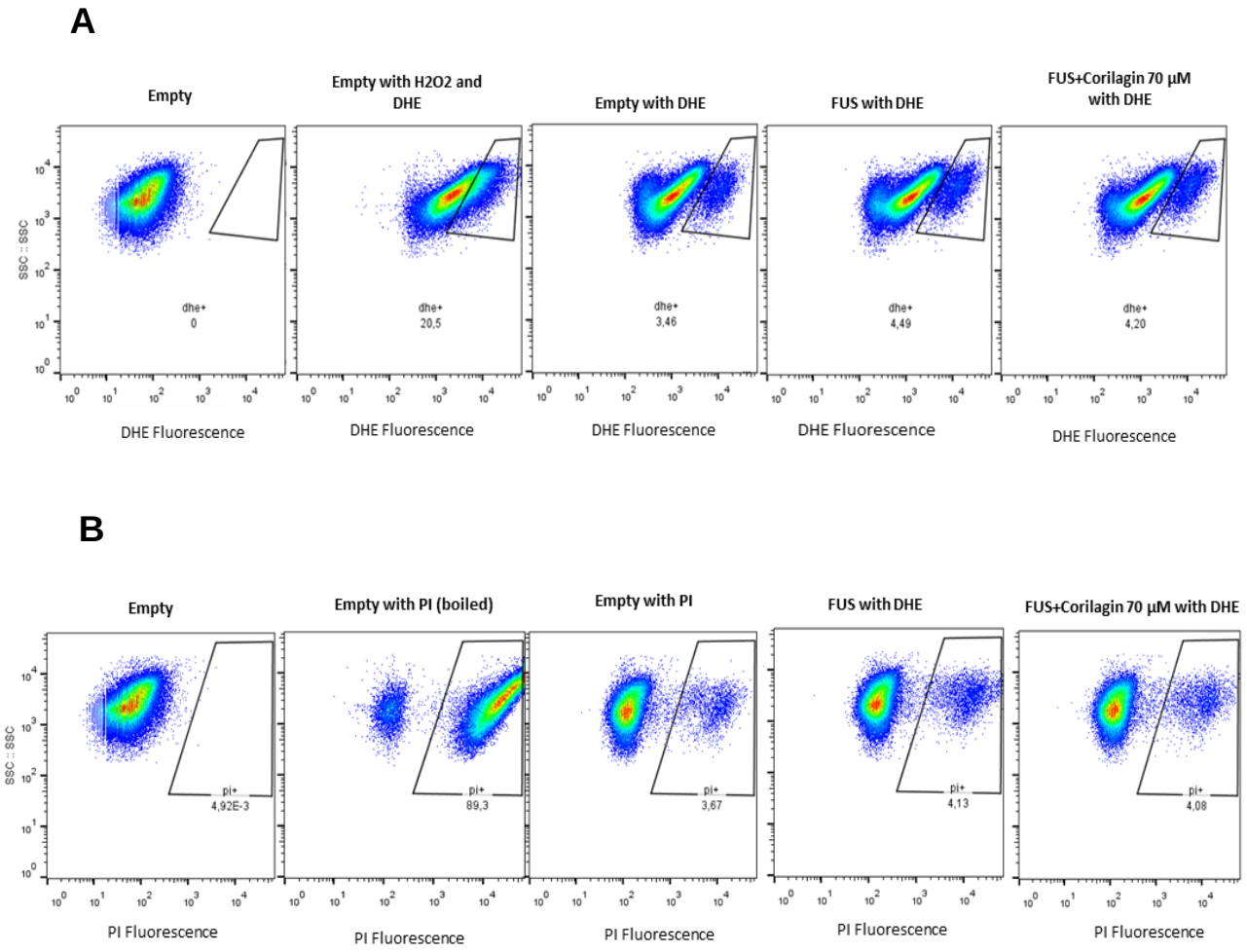

Figure VI.1- Superoxide levels and cell viability assessed by FCM after 6 h of FUS expression and incubation of 70 µM corilagin. (A) Superoxide levels were assessed by dihydroethidium (DHE) fluorescence versus side scatter (SSC). Empty cells were subjected to 500 mM of H_2O_2 and incubated with DHE for 15 min as positive control (B) Viability were assessed by propidium iodide (PI) fluorescence versus SSC. Empty cells were incubated with PI and boiled for 10 min as positive control.

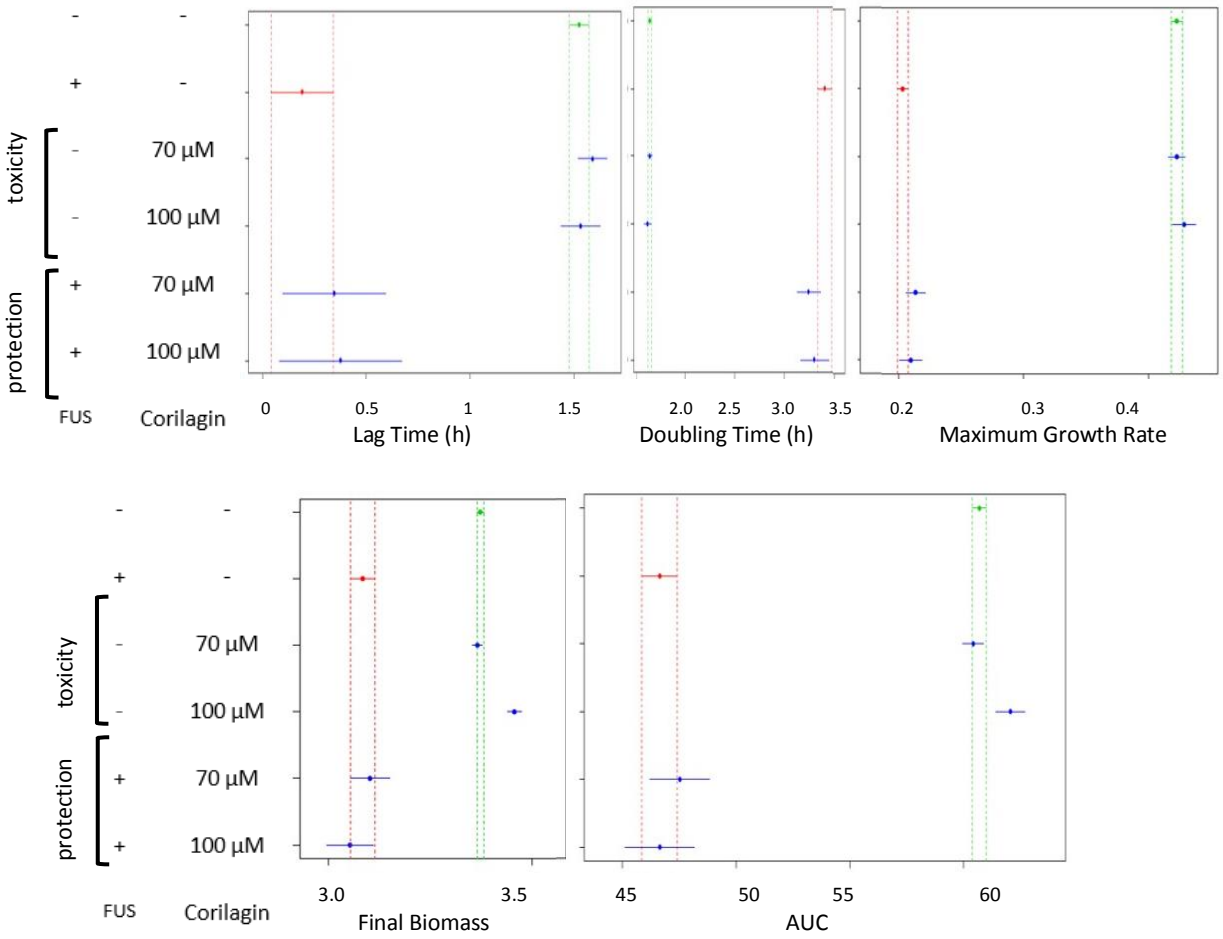

Figure VI.2- Effect of corilagin in cellular growth. The cultures were diluted in SC-URA galactose medium and incubated for 24 h. The 95% confidence interval for BY4741_Sec13-RFP (green) and BY4741_Sec13-RFP_GFP-FUS (red). The growth parameters lag time, doubling time, maximum growth rate, final biomass and AUC, were calculated using the "R" script.

A

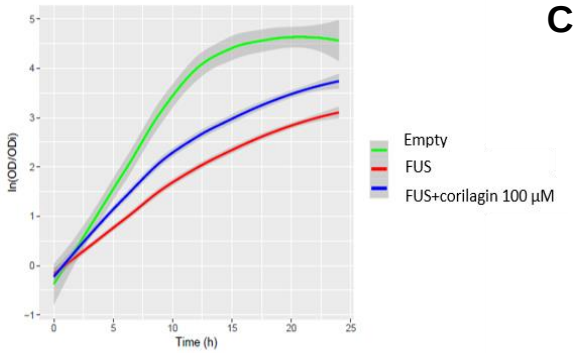

C

Condition Corilagin	Protection factor %	P_Lower Bound	P_Upper Bound
70 µM	22.5	5.7	34.8
100 µM	36.8	25.4	45.1

B

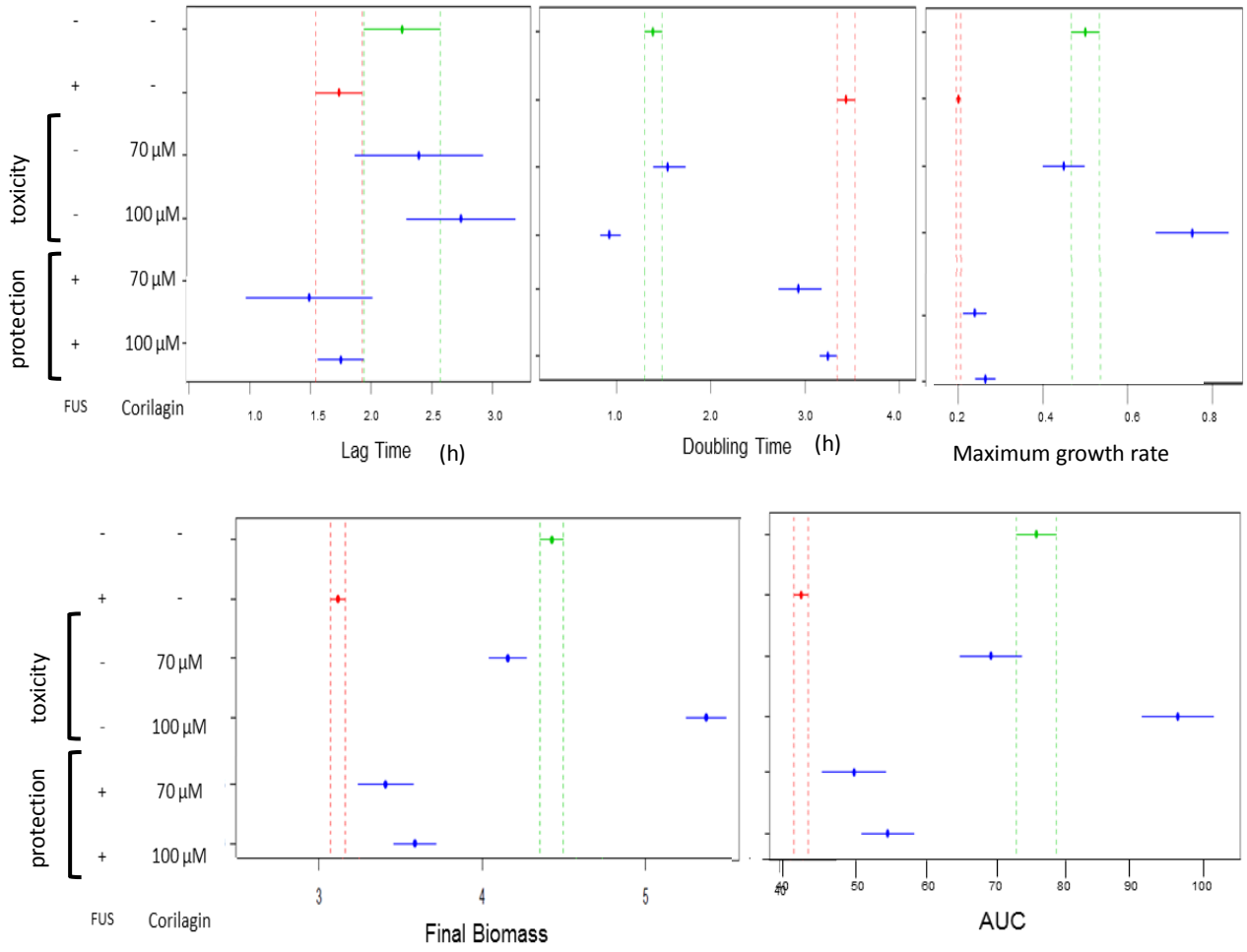

Figure VI.3- Effect of corilagin in cellular growth (A) Growth curves of BY4742 (green), BY4742_GFP-FUS (red) strain incubated with 100 µm corilagin (blue). The cultures were diluted in SC-URA galactose medium for 24 h (B) The 95% confidence interval for BY4742 (green), BY4742_GFP-FUS (red), the growth parameters lag time, doubling time, maximum growth rate, final biomass and AUC, were calculated using the "R" script (C) The protection factor was calculated based on equation on page 14.